MNRAS 000, 1–23 (2024) Preprint 22 October 2025 Compiled using MNRAS LATEX style file v3.0

Modeling 127 solar-like oscillating planet hosts: metallicity threshold for the planetary systems and age-metallicity relation

M. Yıldız*, A. Demirkol, S. Örtel, T. Çakır Alsaç and T. Daylan
Department of Astronomy and Space Sciences, Faculty of Science, Ege University, 35100 İzmir, Turkey.

Accepted XXX. Received YYY; in original form ZZZ

ABSTRACT

We compiled data for 127 hosts (plus six candidates) and used them as constraints to construct interior models of the hosts using the MESA code. Two significant conclusions emerge from these models. First, except for a few stars, the hosts' metallicity (Z_0) is greater than 0.008. This suggests a possible suppression of the occurrence of planets below $Z_0 \approx 0.008$. Second, it concerns how chemical evolution unfolds in the galactic disk. For a given Z_0 value, considering the oldest stars, there is a linear relationship between Z_0 and age (t_9). This line is around t_9=13.4 Gyr at Z_0=0, a value consistent with the age of the Galaxy. The linear relationship continues until around t_9=6 Gyr, and the maximum value of Z_0 remains constant between t_9=2-6 Gyr. Another critical outcome of this study is the discovery of the relationship between Z_0 and the observed metallicity (Z_s) for the hosts. We obtain a useful expression for Z_0, the input parameter for the models, as a function of stellar mass, radius, and Z_s. This expression can be used to estimate Z_0 based on the reduced surface metallicity due to microscopic diffusion. We also derive an expression for planetary mass relative to the orbital semi-major axis and host mass. This expression may indicate a mass distribution near the inner disk where these planets formed, except for hot-Jupiters. Planet radii appear to depend on the planet's mass and irradiation energy, as well as the orbital period.

Key words: stars: planetary systems, planets and satellites: general, stars: oscillation, stars: interior, stars: evolution, planets and satellites: formation

1 INTRODUCTION

Understanding and modeling the internal structures of stars is crucial to astrophysics. While traditional methods like spectroscopy and photometry provide valuable insights into stars, they become less effective as we probe deeper into a star's interior. This is where asteroseismology emerges as a revolutionary technique. Asteroseismology, the study of seismic waves within stars, has become an essential tool in astrophysics, providing invaluable knowledge of stellar dynamics. Many stars display oscillatory behavior. These oscillations lead to periodic variations in their brightness as they expand and contract. For Sun and solar-like stars, oscillations are driven by convective processes that occur in their outer layers.

Fortunately, solar-like oscillations have been detected in many host stars, primarily from the light curves provided by recent space missions such as ESA's Convection, Rotation, and planetary Transits (CoRoT; Baglin et al. 2006), NASA's Kepler/K2 (Borucki et al. 2010; Howell et al. 2014), and the Transiting Exoplanet Survey Satellite (TESS; Ricker et al. 2015). In this study, we compiled asteroseismic and non-asteroseismic data of 133 solar-like oscillating stars and their planets from the literature. 6 of them are planet candidate systems (KOI-5/KIC 8554498, KOI-75/KIC 7199397, KOI-268/KIC 3425851, KOI-364/KIC 7296438, KOI-974/KIC 9414417, KOI-2640/KIC 9088780). We did not remove these stars, but we listed them separately. We examine how asteroseismology plays a key role in studying planetary systems and its importance in enhancing our understanding of these stars. Similar studies are available in the literature (Huber et al. 2013; Kayhan, Yıldız, & Çelik Orhan 2019). These studies are based on a detailed modelling of the hosts and host candidates.

At the beginning of this study, approximately 40 hosts were compiled from the literature. With newly published studies, this number first increased to 80, and then to 127. A recent study by Lin et al. (2025) lists asteroseismic data for 142 hosts and computes fundamental properties of hosts and then planets using the asteroseismic scaling relations. Because the updates are endless, we had to stop at some point. 97 of the 142 hosts are available in our catalog.

The hosts in which planetary systems form and the extent to which planets' properties depend on their host mass, for example, are key questions. How planets evolve, both structurally and orbitally, is also a key question to answer.

Asteroseismology has become a significant tool not only for analyzing the internal structure of stars but also for advancing exoplanet science. To thoroughly investigate planetary systems, it is crucial to understand the structure and evolution of the host star. The more accurately we can determine the properties of the host star, the better we can assess the parameters of the orbiting planets. Asteroseismology enables us to determine stellar parameters with great precision, allowing us to study planets in greater depth.

To this end, two fundamental asteroseismic quantities are significant: the value of the large frequency separation between oscillation frequencies ($\Delta\nu$), and the frequency of maximum amplitude (ν_{max}).

* E-mail: mutlu.yildiz@ege.edu.tr

$\Delta\nu$ is defined as the frequency difference between modes of equal spherical degree ℓ, and consecutive radial orders n. This quantity is intrinsically linked to the acoustic travel time within the star and is approximately proportional to the square root of the mean stellar density (Tassoul 1980; Christensen-Dalsgaard 1993). $\nu_{\rm max}$ scales approximately as $g/\sqrt{T_{\rm eff}}$, where g is the surface gravity (Brown et al. 1991; Kjeldsen & Bedding 1995). As stars evolve and surface gravity decreases, $\nu_{\rm max}$ shifts toward lower frequencies.

The mean of $\Delta\nu$ ($\langle\Delta\nu\rangle$) and $\nu_{\rm max}$ play an important role in determining the mass (M) and radius (R) of oscillating stars. The standard asteroseismic scaling relations, which allow the estimation of the radius ($R_{\rm sca}$) and mass ($M_{\rm sca}$) of an oscillating star, are given as follows:

$$\frac{R_{\rm sca}}{\rm R_\odot} = \frac{\nu_{\rm max}/\nu_{\rm max\odot}}{(\langle\Delta\nu\rangle/\langle\Delta\nu_\odot\rangle)^2}\left(\frac{T_{\rm eff}}{\rm T_{eff\odot}}\right)^{1/2}, \quad (1)$$

$$\frac{M_{\rm sca}}{\rm M_\odot} = \frac{(\nu_{\rm max}/\nu_{\rm max\odot})^3}{(\langle\Delta\nu\rangle/\langle\Delta\nu_\odot\rangle)^4}\left(\frac{T_{\rm eff}}{\rm T_{eff\odot}}\right)^{3/2}. \quad (2)$$

Here, $\langle\Delta\nu_\odot\rangle$ and $\nu_{\rm max\odot}$ correspond to the solar values and the adopted values of $\langle\Delta\nu_\odot\rangle$ = 135.1 μHz and $\nu_{\rm max\odot}$ = 3090 μHz (Sharma et al. 2016).

The small frequency separation ($\delta\nu$) is another crucial asteroseismic parameter (Christensen-Dalsgaard 1988). It is defined as the frequency difference between modes of consecutive radial order n and with a degree difference of two. The $\delta\nu_{02}$, calculated from modes with $l = 0$ and $l = 2$, is highly sensitive to the conditions in the stellar core during the main-sequence phase (MS), making it a valuable age indicator. As a star evolves along the MS, $\delta\nu_{02}$ decreases, being about 15 μHz at the zero-age main sequence (ZAMS) and around 5 μHz near the terminal-age main sequence (TAMS). For the Sun, $\delta\nu_{02}$ has a value of 9.8 μHz (Yıldız, Çelik Orhan, & Kayhan 2016), which indicates that it is roughly halfway through its MS lifetime.

In this study, we analyze host stars at different evolutionary stages. Only a few of the solar-like oscillating host stars in the literature are MS stars. The vast majority are subgiant (SG) and red giant (RG) or red clump (RC) stars. Both the different structures of stars at different evolutionary stages and the fact that non-asteroseismic observational data, especially, have different uncertainty levels prevent us from applying a single modeling method. Therefore, it would be more useful to apply the technique based on each star's observational data. We used $\Delta\nu$ and surface metallicity ($Z_{\rm s}$) constraints for each star. We also used the reference frequencies ($\nu_{\rm min0}$, $\nu_{\rm min1}$ and $\nu_{\rm min2}$), effective temperature ($T_{\rm eff}$), luminosity (L), and R calculated from the scaling relations as constraints according to the uncertainty level in the data of the stars. Analyzing the results obtained by applying several methods to some hosts would help us decide which method we prefer.

Detailed models of host stars are essential for many reasons: 1) good determination of the mass and radius of the stars allows good determination of the mass ($M_{\rm p}$) and radius ($R_{\rm p}$) of the transiting planets, 2) the initial chemical composition of the star affects its own structure and also represents the chemical composition of the environment in which the planet formed, 3) the age, which we can determine more precisely, especially with asteroseismic data, also reveals how the planets have evolved from the time they formed to the present.

It is also interesting that there are stars in the RC phase among the hosts. It is well known that the star loses a significant amount of mass as it climbs the RG branch, approximately 0.1-0.3 $\rm M_\odot$ (Lebzelter & Wood 2011; Miglio et al. 2012). In cases where there is such a mass loss, the planet is greatly affected for two reasons: 1) Since the central body loses mass, there is a significant change in the planet's orbit, 2) some of the mass lost by the star can be directly transferred to the planet, and in this case, the structure of the planet can change significantly. Such processes are complex, and depending on how mass accretion occurs, different outcomes can result. Perhaps the most important result for humanity is that even some stars in the RC phase still have planets orbiting them.

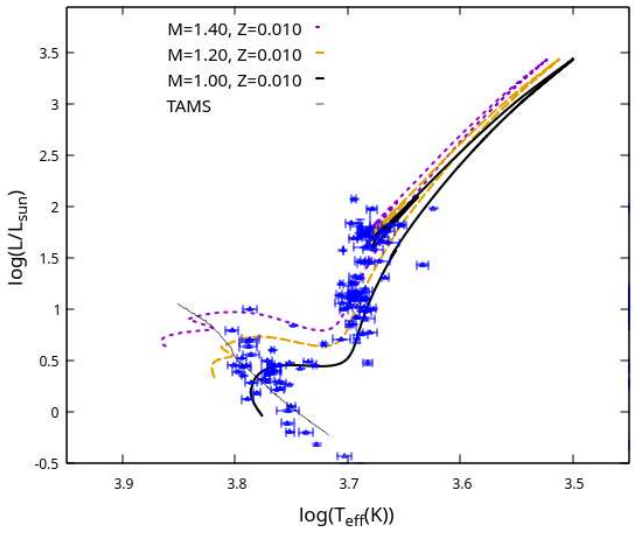

Figure 1. The classical HRD of the oscillating host stars. The thick solid and dashed lines represent the evolutionary tracks at Z = 0.0100 for 1.0, 1.2, and 1.4 $\rm M_\odot$. The thin solid line denotes the TAMS.

The paper is organized as follows: Section 2 presents the observed properties of the host stars and their planetary systems. Section 3 describes the modelling methodology adopted in this study. The results of the computations are presented and discussed in Section 4. Finally, Section 5 provides the main conclusions of this study.

2 OBSERVED PROPERTIES OF THE HOSTS AND THE PLANETARY SYSTEMS

The search for life on planets other than Earth, a highly popular field of research today, has led to a much more detailed study of planetary systems. In this study, knowledge of host stars, in particular, facilitates the study of planets. This is because the more we know about the host star, the more information we can obtain about the planet. Therefore, asteroseismology, the most effective method for explaining the internal structure and evolution of stars, has become an essential tool in the study of planetary systems. We compiled asteroseismic and spectroscopic data of systems containing planets from the literature (Table A1).

2.1 Non-asteroseismic properties of the planetary systems

The luminosities of the stars in Table A1 are primarily obtained from references using GAIA DR3 and DR2 data (Gaia Collaboration et al. 2018, 2021). Many studies provide [Fe/H] and $T_{\rm eff}$ values for many of the hosts. Generally, these values are quite scattered. In this case, we tried to construct interior models for a host and obtain the observational data that best fit its model. The Hertzsprung–Russell diagram (HRD) plotted from the compiled data is shown in Fig. **??**.

According to the TAMS line (Yıldız 2015), around 15 planet hosts are MS stars. Nearly 25 hosts are SGs, and the remaining 127 hosts are RGB stars. There may be a small number of core-helium-burning (CHeB) stars among the stars in the RGB. Masses of the hosts range from 0.75 to 2.66 $M_\odot$. The radius interval is about 0.75-15 $R_\odot$.

[Fe/H] (or [M/H]) and $T_{\rm eff}$ of the hosts are obtained from the spectroscopic data. [Fe/H] or [M/H] represents metallicity of the photosphere of the hosts ($Z_{\rm s}$). For the interior models, however, the initial metallicity (Z_0) is the input parameter. For the evolved stars, Z_0 can be taken as $Z_{\rm s}$. However, for the hosts on and around MS, $Z_{\rm s}$ may significantly be less than Z_0, due to microscopic diffusion, depending on the age and depth of the stellar convective envelope. The $Z_{\rm s}$ of the planet hosts are computed from the [Fe/H] or [M/H] values:

$$Z_{\rm s} = 10^{[\rm Fe/H]} Z_\odot,$$

where $Z_\odot$ is the solar metallicity and taken as 0.0134 (Asplund et al. 2009). For two of the hosts, namely KIC 6278762 and TIC 160224839, $Z_{\rm s}$ is small, ~ 0.005. For most of the stars, the metallicity ranges from -0.3 to 0.3 dex. This implies that $Z_{\rm s}$ for most of the systems varies between 0.007 and 0.027.

As part of our study, we examined 127 planetary systems and 179 planets. We compiled the masses, radii, orbital periods, and semi-major axis lengths of the planets from the literature to create a catalog. In our sample, planetary masses range from 22 $M_{\rm J}$ to 0.0001 $M_{\rm J}$, while radii span 1.36 $R_{\rm J}$ to 0.036 $R_{\rm J}$. A total of 27 multi-planet systems are identified. Since asteroseismology allows us to determine the fundamental parameters of host stars with high precision, the properties of their planets can also be constrained with great accuracy. Therefore, these systems are of particular importance for studying planetary evolution and characterizing their fundamental properties (Section 4.6-4.8).

2.2 Asteroseismic properties of the hosts

The asteroseismic properties of the majority of planet hosts have been published in several studies (Appourchaux et al. 2012; Huber et al. 2013; Silva Aguirre et al. 2015; Davies et al. 2016; Kayhan, Yıldız, & Çelik Orhan 2019; Zhou et al. 2024). The quality of observational data of each planetary system and the number of observables are quite different from the others. While for some stars the available asteroseismic data include only their $\Delta\nu$, some of them have individual oscillation frequencies for many modes. Determining many oscillation frequencies is important because we can then use the reference frequencies as constraints. The asteroseismic properties of the Kepler RC and RG targets are given in the APOKASC-2 catalogs. $\nu_{\rm max}$ and $\Delta\nu$ of the TESS targets are mainly published in references. $\nu_{\rm max}$ of the hosts is plotted with respect to $\Delta\nu$ in Fig. 2a. $\Delta\nu$ of RC and RGB stars ranges 2.5-8.8 and 0.45-18.7 μHz, respectively. $\nu_{\rm max}$ of RC and RGB stars range 18.6-115 and 2.02-246.7 μHz, respectively.

During the RGB phase, stars rapidly lose significant mass, increasing their radius, and then undergo a helium flash, entering the RC region. RGB stars have radii as high as 51 $R_\odot$, while RC stars have radii in the range of 8-21 $R_\odot$. This means that planets closer to their hosts than 50-60 $R_\odot$ are likely to be engulfed, unless something happens to them before then. TIC 233008631 is the host with its smallest values for $\Delta\nu$ and $\nu_{\rm max}$: $\Delta\nu = 1.79 \pm 0.05$ and $\nu_{\rm max} = 10.4 \pm 1.7$. In Fig. 2b, the uncertainty of $\Delta\nu$ and $\nu_{\rm max}$ values is plotted as a percentage. The stars with the highest uncertainties in their asteroseismic data are TIC 332711151 and TIC 77481104.

If a host is an RC star, then the period spacing ($\Delta\Pi_1$) is a significant constraint to model the interior of a star. Unfortunately, $\Delta\Pi_1$ is not

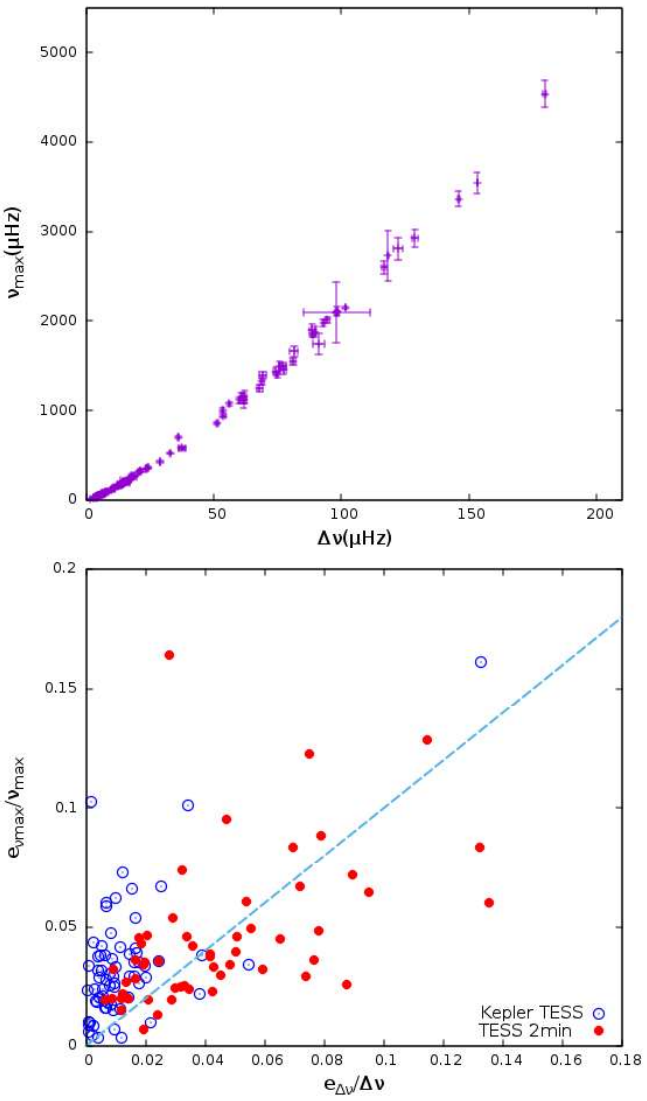

Figure 2. a) $\nu_{\rm max}$ is plotted with respect to $\Delta\nu$. b) Uncertainty of $\nu_{\rm max}$ is plotted with respect to $\Delta\nu$.

available for any host taking place in the RC region in Fig. 3. In Fig. 3, $\nu_{\rm max}$ is plotted against $\Delta\nu$ for the host stars and compared with RGB and RC stars from the APOKASC-2 sample. The majority of the host stars are located near the RC sequence. Whether these stars are truly RC objects or appear to be so due to associated uncertainties remains a matter of debate and requires further investigation.

The $\delta\nu_{02}$ values have been determined for 16 of the MS and SG stars, ranging from 4.3 to 9.0 μHz. $\nu_{\rm min0}$ and $\nu_{\rm min1}$ obtained from the $\Delta\nu$–ν plot are determined for 23 of the 133 host stars. For 6 stars, either $\nu_{\rm min0}$ or $\nu_{\rm min1}$ is detected. $\nu_{\rm min0}$ and $\nu_{\rm min1}$ have values in the ranges 245-4221 μHz and 552-3849 μHz, respectively.

3 METHOD OF MODELLING

Instead of applying a single method to all stars during modeling, we used different methods based on the data in the literature and their uncertainties. The asteroseismic data must be of high quality. Stars with detected individual oscillation mode frequencies are the most advantageous stars. In this case, we know that the model we

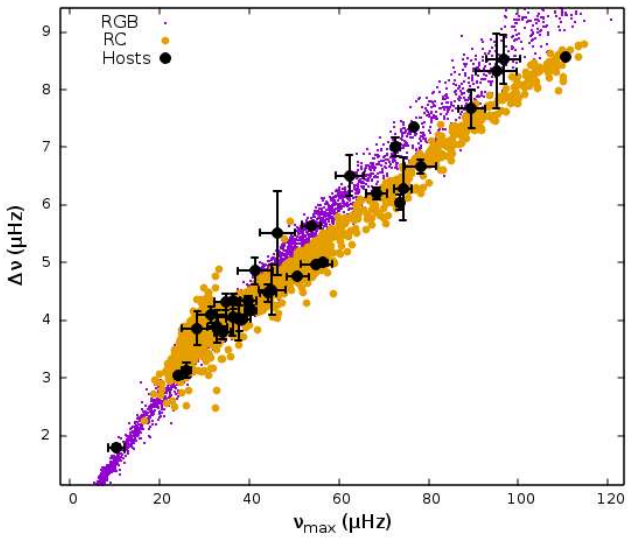

Figure 3. $\Delta\nu$ is plotted with respect to ν_{max} for hosts to compare with RGB and RC stars in APOKASC-2. In this diagram, RC and RGB stars are slightly separating. Some of the hosts are likely RC stars.

obtained by using $\Delta\nu$, reference frequencies, and Z_s as constraints is the unique model (Örtel et al. 2025). This method is called MinZ.

We can find the masses and radii of stars using asteroseismic scaling relationships. In this way, the masses calculated in particular are highly uncertain. There are three important disadvantages of using ν_{max} in the scaling relations, especially for MS and SG stars. First, we cannot correct the relation of ν_{max} to the fundamental stellar parameters of the models. Second, multiple maxima can be observed in the power spectrum of hot F-type stars. Third, the uncertainty in ν_{max} is generally higher than the uncertainty in $\Delta\nu$: $e_{\nu_{max}}/\nu_{max} = 6e_{\Delta\nu}/\Delta\nu$. For the TESS 2min cadence light curves (Zhou et al. 2024), $e_{\nu_{max}}/\nu_{max}$ and $e_{\Delta\nu}/\Delta\nu$ are high and close to each other. When we compare TESS and Kepler targets, we see that Kepler data have less uncertainty. For Kepler target stars, $e_{\Delta\nu}/\Delta\nu < 0.05$ and $e_{\nu_{max}}/\nu_{max} < 0.02$.

The chemical composition of a star is among the most influential initial essential properties. Metallicity, in particular, significantly affects the structure of the nuclear core and the outer regions. Therefore, it is one of the most important ingredients of the interior models, after the stellar mass. In all the methods for asteroseismic modelling, we first use Z_0 calculated from the observed metallicity of the hosts. According to the difference between Z_0 and Z_s, we estimate a new Z_0. For the evolved RGs, Z_0 is close to Z_s. For the stars with high-quality spectroscopic and asteroseismic data, Y_0 and α can be computed by calibrating the models under the observational constraints. This is the case for most of the hosts with reference frequencies. We call this method Method DZref.

If the oscillation frequencies of the individual modes are not available in the literature, we compute $\Delta\nu$, Z_s, and T_{eff} as the observational constraints (Method DZT). For some stars, the spectroscopic T_{eff} is quite uncertain. In such cases, we either use luminosity derived using GAIA data (Method DZL) or radius computed from the scaling relations (Method DZR). For Methods DZT, DZL, and DZR, we assume that the chemical enrichment on the galactic disk proceeded as an increase in Y (ΔY) is twice the increase in Z (ΔZ): $\Delta Y = 2\Delta Z$. Then, $Y = Y_p + 2Z$, where $Y = Y_p$ and $Z = 0$ for the first stars in the Galaxy. The primordial Y_p value is determined by the Planck collaboration (Planck Collaboration et al. 2020) as 0.2471.

In the HRD, the RC region is narrow and perhaps the most degenerate region. Since the stars in this region are not located in a sequence, unlike in the MS, many model options exist for a given mass and chemical composition. Therefore, instead of performing precise calibrations in the first stage for RC candidates, we can consider the system age as the age of the primary component in the RG branch.

First, we compute the fundamental stellar parameters using the modified scaling relations. Then, we compare these results with the model results with the closest values of Z and M in the HRD. If there is a good agreement, then this model is the best model for the host star. If not, we test other mass and Z combinations.

3.1 Properties of MESA evolution code

Nonrotating interior models of the planet hosts are constructed using MESA code version r23.05.1 (Paxton et al. 2011, 2013, 2015, 2018, 2019; Jermyn et al. 2023). Element diffusion is applied using the method proposed by (Paquette et al. 1986) for the stars with M< 1.4 $M_\odot$. For the higher masses, the models are without diffusion. The standard mixing length theory proposed by Böhm-Vitense et al. (1958) is used for the convection. The opacity is computed using OPAL tables (Iglesias & Rogers 1993, 1996) at high temperature and the tables of Ferguson et al. (2005) at low temperature. Depending on the current state of evolution of the stars, the internal structure models cover pre-MS, MS, SG, and RG phases.

In MESA, different equations of state (EOS) are blended depending on the temperature–density regime (Paxton et al. 2011, 2013, 2015, 2018, 2019). For the stars studied here (MS, SG, and RGB phases), most of the stellar models lie within the regime covered by FreeEOS[1].

The adiabatic oscillation frequencies of the fitted model are computed using the ADIPLS package (Christensen-Dalsgaard 2008). To account for the surface effect, the correction proposed by Kjeldsen, Bedding, & Christensen-Dalsgaard (2008) is applied.

4 RESULTS AND DISCUSSIONS

4.1 Model properties across the observed properties

In Fig. 4a, the observed large frequency separation ($\Delta\nu_{obs}$) of the host stars is compared with the model values ($\Delta\nu_{mod}$). $\Delta\nu_{mod}$ shows an excellent match with $\Delta\nu_{obs}$, confirming the reliability of the modelling.

Fig. 4b shows the comparison between observed (T_{obs}) and modelled effective temperatures (T_{mod}). Overall, T_{obs} and T_{mod} are in perfect agreement, although some scatter is visible. This scatter is likely due to the relatively significant uncertainties in the observed stellar temperatures.

4.2 Asteroseismic HR Diagram

The age of a star is a key parameter for understanding its internal structure and the evolution of stellar and planetary systems. Asteroseismology enables the determination of stellar ages with significantly higher precision than other methods. An asteroseismic HRD is an effective tool for this purpose (Christensen-Dalsgaard 1993).

[1] https://freeeos.sourceforge.net/

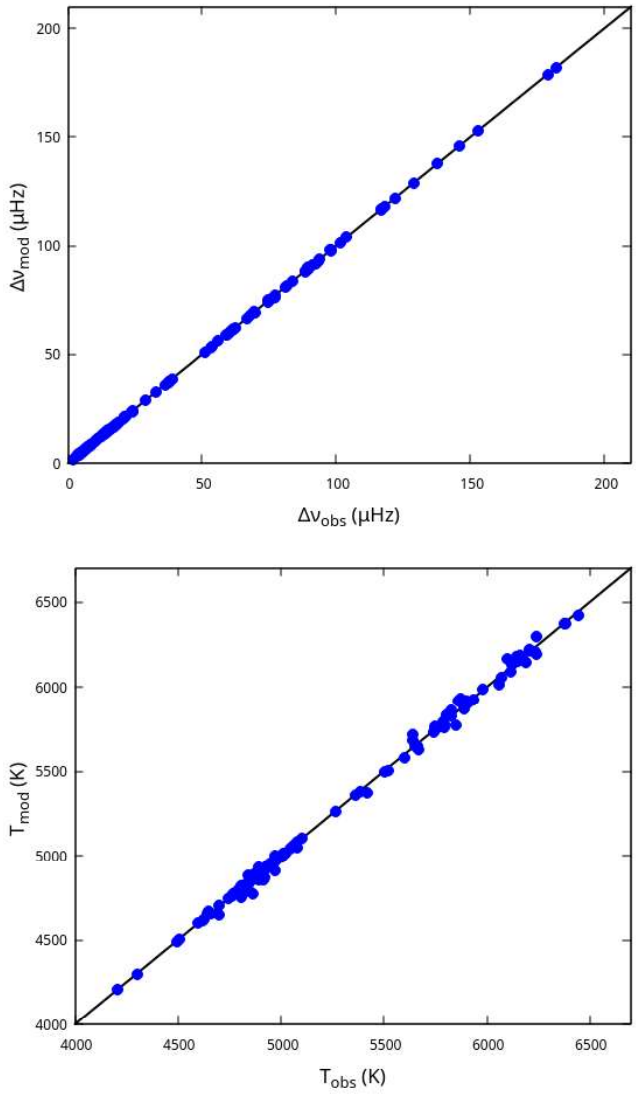

Figure 4. a) $\Delta\nu_{\rm mod}$ is plotted with respect to $\Delta\nu_{\rm obs}$. b) $T_{\rm mod}$ is plotted with respect to $T_{\rm obs}$.

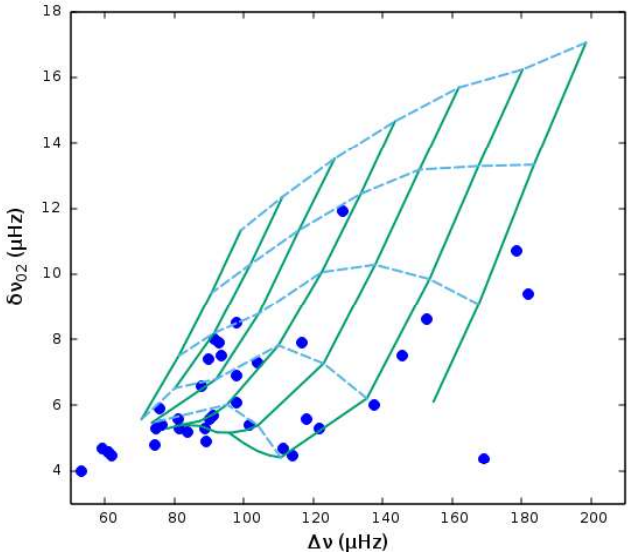

Figure 5. Asteroseismic HRD for models of the hosts. The grids are prepared for $M = 0.8-1.4\,{\rm M}_\odot$ and $Z_0 = 0.02$ (nearly vertical solid lines). The dashed lines show the evolutionary phases from ZAMS (at the top) to TAMS (at the bottom).

In Fig. 5, the $\Delta\nu$ is plotted against the small frequency separation to construct an asteroseismic HRD for the host star models. In this diagram, solid lines indicate stellar mass (1.2 $M_\odot$ on the left and 0.8 $M_\odot$ on the right), while dashed lines indicate the MS phases (ZAMS at the top and TAMS at the bottom). The stars form two clear groups: one is concentrated near the TAMS, while the others appear to have completed about three-quarters of their main-sequence lifetime.

4.3 Metallicity-age relationship

The Z_0-t_9 relationship obtained from host internal-structure models is shown in Fig. 6. This figure shows two interesting features. One of these is about galactic chemical evolution: For stars formed from gas clouds with the fastest increasing metallicity, there is a linear relationship between Z_0 and $t_0 = t_{\rm MW} - t_9$. $t_{\rm MW}$ is taken as 13.4 Gyr (Pasquini et al. 2004).

Old stars formed in the early epochs of the Milky Way generally exhibit lower metallicities, while younger stars exhibit higher metallicities. This trend is consistent with expectations from galactic chemical evolution. Another critical point is that no planetary systems are found below a certain metallicity threshold. In our samples, we observe that host stars with $Z_0 < 0.008$ do not harbor planetary systems. This may be the main link between stellar metallicity and the occurrence of planetary systems. Hence, this aspect plays a crucial role in studying stellar–planetary evolution and in improving our understanding of planet formation processes.

KIC 6278762's position in this figure is far from the other stars. The observed metallicity is quite low, approximately 0.005. The age of the model (14.6 Gyr) we obtain from the observed values is greater than the age of the Galaxy. As we increase Z_0 and decrease $\Delta\nu$, the KIC 6278762 model approaches the models of the other stars. The nearest model has a Z_0 of 0.0104 and a $\Delta\nu$ of 179.3 μHz. The situation of this low-mass star can also be considered in relation to the opacity enhancement observed when examining cool stars.

4.4 The initial metallicity versus surface metallicity

Because more energy is expended on ionization when the number of heavy elements is high, less of the energy gained from the collapse during star formation is spent on heating the deep interior. In this case, the temperature increases less, leading to slower nuclear reactions and lower luminosity. From this perspective, the initial Z has a significant impact on the structure of stars (especially their luminosity). Z, determined from spectral observations, is actually the surface heavy element abundance $Z_{\rm s}$. Structure and evolution, in turn, depend primarily on Z_0. The crucial question here is whether we can calculate Z_0 from $Z_{\rm s}$.

Using the data of host interior models, the fractional difference $\delta Z/Z_{\rm s}$ $((Z_0 - Z_s)/Z_s)$ is plotted against R in Fig. 7a. The difference is particularly significant for the range $R < 3\,{\rm R}_\odot$. For larger radii, the deepening convective envelope eliminates the chemical separation caused by microscopic diffusion. For $R < 3\,{\rm R}_\odot$, R roughly represents the evolutionary state. Diffusion effect depends on the depth of the convective envelope. The depth of the convective envelope depends

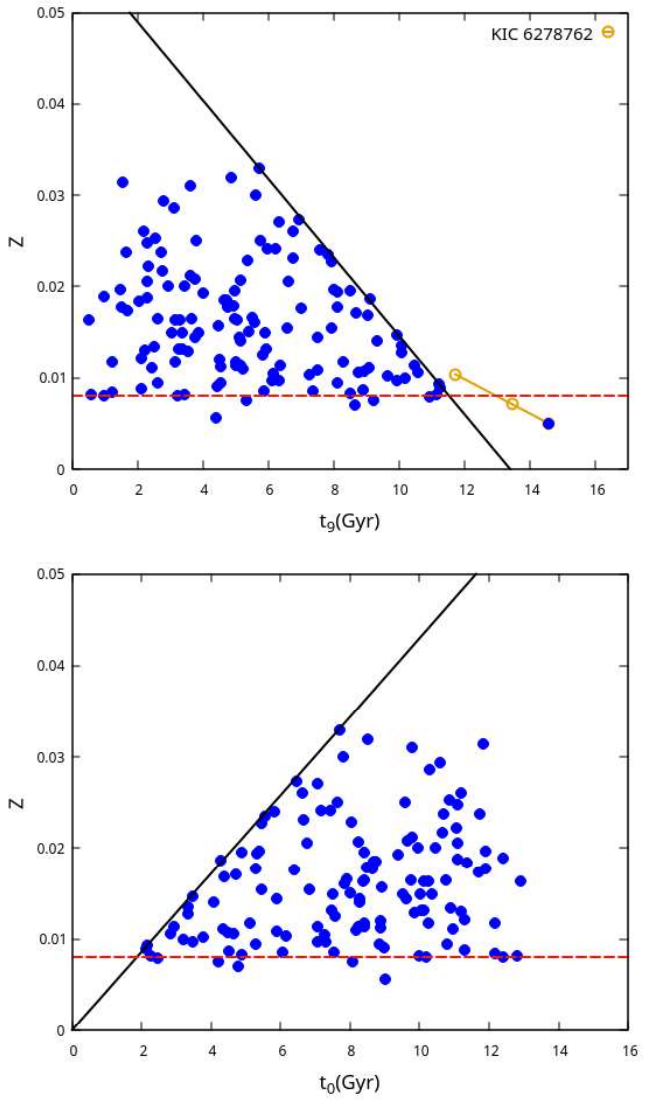

Figure 6. Z_0 is plotted with respect to age. The solid line is the border for the stars with the highest metallicities of their ages, expressed as $Z = -0.00395t_9 + 0.053$. KIC 6278762 (circle) stands apart from the other stars. Opacity enhancement may be a solution to this problem (see the text).

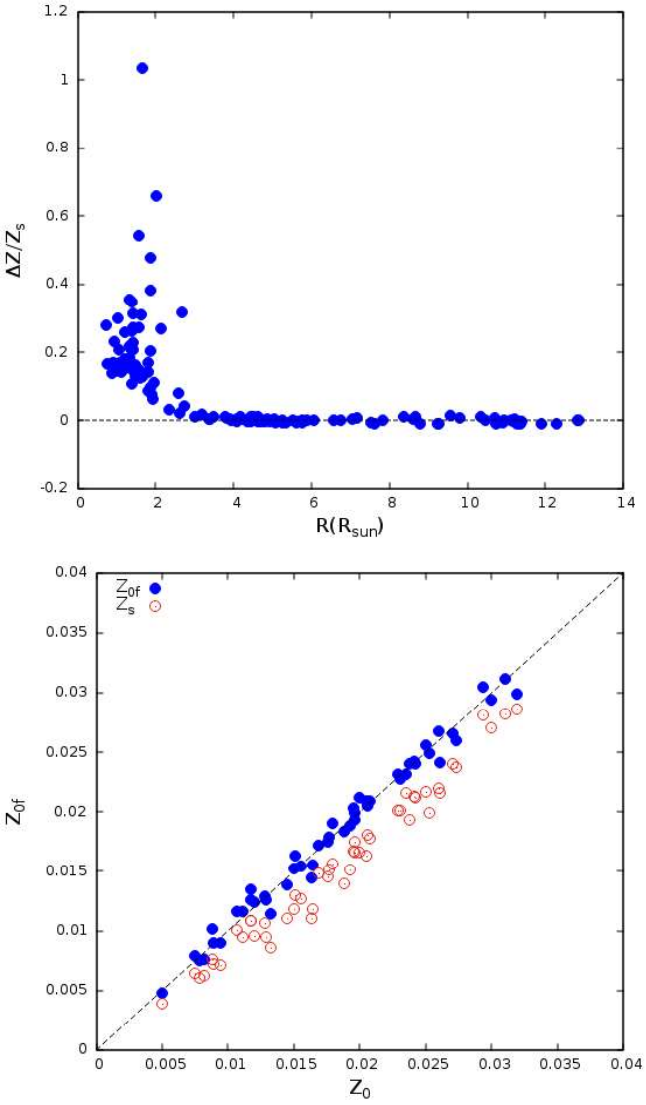

Figure 7. a) The fractional difference between Z_0 and Z_s is plotted with respect to radius for the interior models of the hosts. This difference is due to microscopic diffusion and is significant for the stars with $R < 3R_\odot$. We obtain a fitting formula assuming the difference is a function of M, Z, and R. b) Z_{0f} (filled circles), computed from the fitting formula, is plotted against the original Z_0. Also plotted is the Z_s (circles).

on M and Z. Then we can consider $\delta Z/Z_s$ as a function of M, Z_s, and R: $f(M, Z_s, R)$. We assume a function as

$$\frac{\delta Z}{Z_s} = f(M, Z_s, R) = b\frac{M}{M_\odot} + cZ_s + d\frac{R}{R_\odot}. \quad (3)$$

From this function, we obtain the fitting formula using the data of 50 hosts for which $dZ > 0.0005$: $\delta Z/Z_s = f = bM + cZ + dR$ Then, we can compute Z_0 in terms of M, Z_s, and R:

$$Z_{0f} = Z_s(1 + f) \quad (4)$$

In Fig. 7b, Z_{0f} is plotted respect to Z_0. The metallicities calculated from the model and the Z_0 relationship are in excellent agreement.

In our host sample, there are a few stars in the vicinity of the ZAMS. Therefore, equation (3) is only valid for evolved MS and SG stars. For the young stars, $\delta Z/Z_s$ is a double-valued function of R.

4.5 Revised radius and mass of the planets

Due to two spheres passing in front of each other, the light curve of a planetary system changes. The transit depth, ΔF, with F defined as the total observed flux, is given as (Seager & Mallén-Ornelas 2003)

$$\Delta F = \left(\frac{R_p}{R}\right)^2. \quad (5)$$

Since the radius ratio will be constant for a given value of ΔF, we can also calculate the revised R_p (R'_p) from the newly calculated R of the host. R'_p is also listed in Table A2. The fractional difference between R'_p and R_p ($(R'_p - R_p)/R_p$) is plotted with respect to R in the upper panel of Fig. 8. The difference is less than 10 per cent.

The revised planetary mass is computed from the ratio of the new stellar mass to the old one. In the lower panel of Fig. 8, the fractional

difference between M'_p and M_p ($(M'_p - M_p)/M_p$) is plotted against R. For most planets, the difference is quite large, reaching up to 50%. This difference is due to the difference between the new stellar mass and the old mass. For TIC 200093173b, the difference is about 55%. The mass of the host is given as 0.98 ± 0.125 $M_\odot$ in Feng et al. (2022) and is found to be 1.517 $M_\odot$ in the present study. It is worth noting that M_p here is mostly $M_p \sin i$.

4.6 Expression for M'_p as a function of a and M

In Fig. 8, M'_p is plotted with respect to M and a in logarithmic scales. The grids shows the fitted function $f(x, y)$:

$$\log\left(\frac{M'_p}{M_J}\right) = (1.10\pm0.07)\log\left(\frac{a}{AU}\right) + (1.39\pm0.37)\log\left(\frac{M}{M_\odot}\right). \quad (6)$$

According to this relationship, the planetary mass increases with increasing M and a. This result is interesting because it may indicate the density that existed under the conditions of the disk (presumably in the inner parts of the disk) that produced the planet with mass M'_p. Other systems in the TEPCat catalog are also plotted for comparison. We observe that hot Jupiters are relatively rare among the b planets of our 127 hosts. Hot Jupiters form a distinct group. This supports the idea that these planets reached their current positions through migration.

4.7 How R_p depends on M_p and orbital parameters?

It is well known that there are three distinct M-R relationships for planetary mass ranges: rocky, Neptune-like, and Jovian. For the latter two in particular, the M-R relationship exhibits significant scattering. The host's irradiation flux plays a significant role in this scattering. A much more precise relationship emerges when the irradiated energy per gram per second (l_-) is used instead of the flux (Yıldız et al. 2014). In addition to these parameters, R'_p shows a secondary dependence on orbital period P. The fitting formula for R'_p (R'_{pfit}) is obtained as

$$\log\left(\frac{R'_{pfit}}{R_J}\right) = (-1.33 \pm 0.20) + (0.290 \pm 0.038)\log\left(\frac{l_-}{l_0}\right) + (0.418 \pm 0.023)\log\left(\frac{M'_p}{M_J}\right) + (0.407 \pm 0.066)\log\left(\frac{P}{day}\right). \quad (7)$$

where l_0 is the energy received per unit mass and time by a planet with 1 M_J and 1 R_J at 1 AU in our Solar system ($l_0 = 1.106 \times 10^{-4}$ erg g^{-1} s^{-1}).

In Fig. 9, R'_{pfit} is plotted with respect to R'_p. The average difference between R'_{pfit} fit and R'_p is approximately 14 percent. The biggest difference is for KIC 8494142b, about 43 percent.

4.8 Notes on individual hosts

4.8.1 16 Cyg B (KIC 12069449)

The asteroseismic data of 16 Cyg B is obtained from Kepler lightcurves (Metcalfe et al. 2012). Its individual oscillation frequencies are derived from this data. Its $\delta\nu_{02}$ is 6.6 μHz and is an essential constraint on age indicators. While its ν_0 is well defined, ν_1 is around the first interval of the data (2044 μHz). Detailed interior models of 16 Cyg A and B are constructed by Metcalfe et al. (2012) using different codes. M, R, and age are found to be 1.07±0.02 $M_\odot$, 1.127±0.007 $R_\odot$, and 6.7±0.4 Gyr, respectively. These models are in good agreement with the asteroseismic and non-asteroseismic data of these stars. Perhaps the low value of Y_0 is controversial. While the

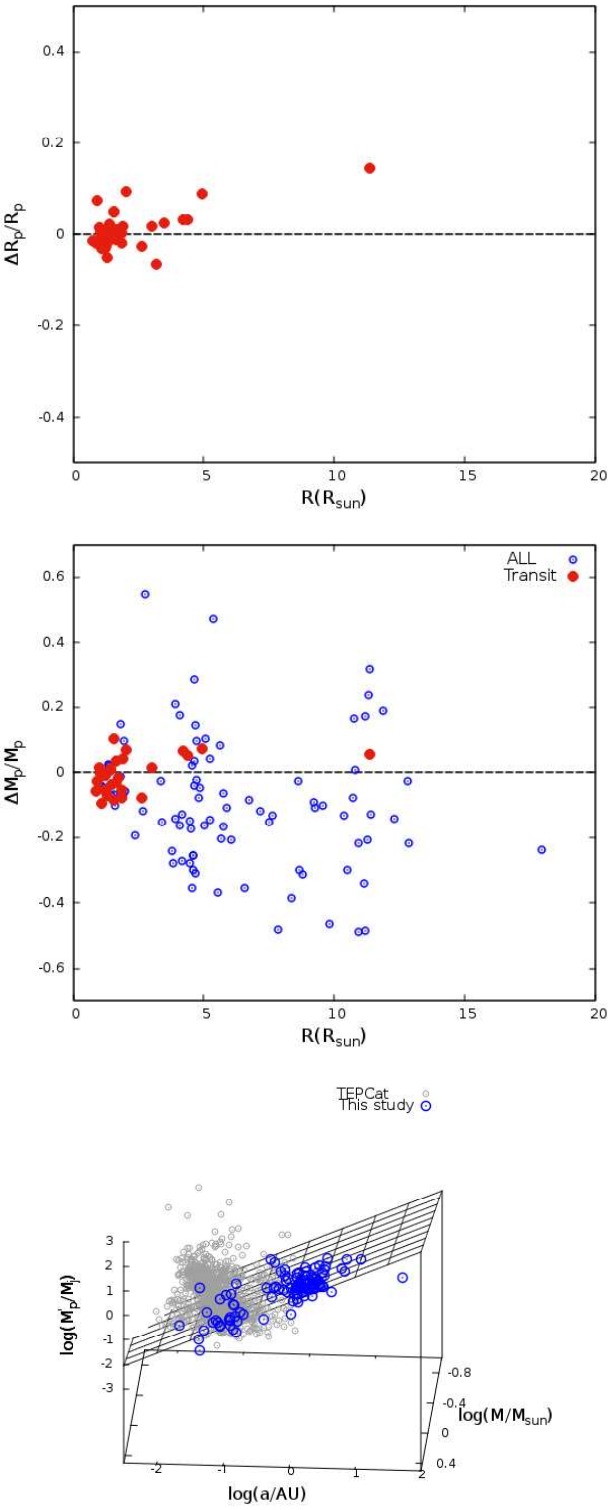

Figure 8. a) $(R'_p - R_p)/R_p$ and b) $(M'_p - M_p)/M_p$ are plotted with respect to R of the hosts. Radii of the transit planets are determined from the observations in units of their host radii (filled circles). The difference for Rp is less than 10 percent for 37 transit planets. For these planets, the difference for M_P is similar to that of R_P. However, for all of the planets (circle), the difference is less than 50 percent. c) In the lower panel, M'_p is plotted with respect to a and M in logarithmic scales.

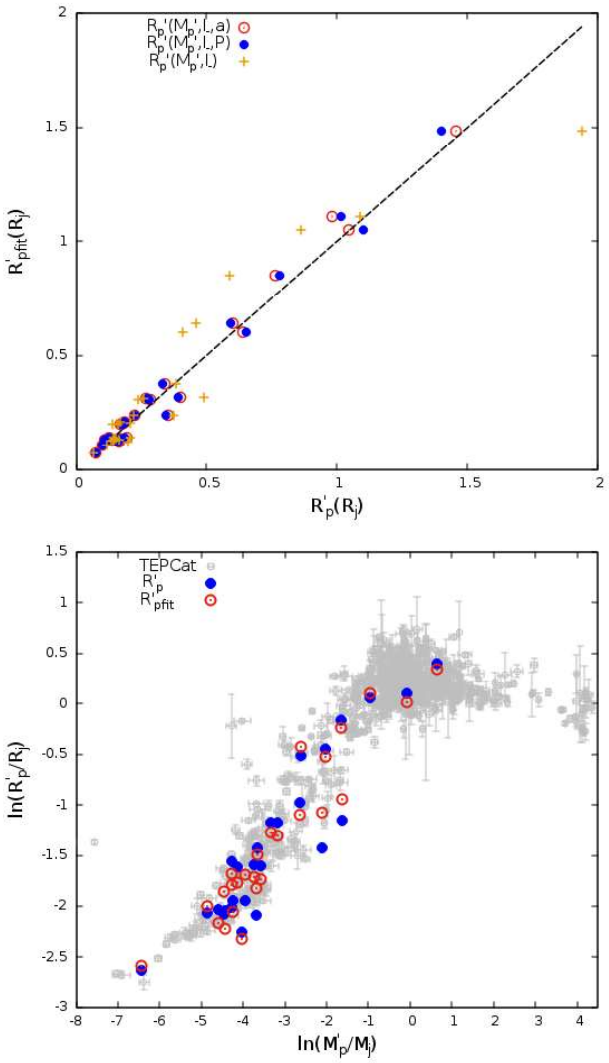

Figure 9. a) $R'_{\rm pfit}$ (filled circle) given in equation (7) is plotted with respect to $R'_{\rm p}$. We obtain another fit for $R'_{\rm p}$ by substituting a (circle) for P in equation (8). The two fits give similar results. To see the direct effect of the orbital parameters, we obtain an expression as a function of $M'_{\rm p}$ and l_- (+). The $R'_{\rm pfit}$ obtained from this expression is not in good agreement with $R'_{\rm p}$. b) $\ln(R'_{\rm p})$ (filled circle) and $\ln(R'_{\rm pfit})$ (circle) are plotted with respect to $\ln(M'_{\rm p})$. For comparison, the planets in TEPCat are also shown (gray errorbars).

adopted Z_0 of 16 Cyg B (0.024) is greater than the solar value, the Y_0 of all models (averaging 0.25) is much smaller than the solar value. This Y_0 is close to the primordial helium abundance (0.2471).

The fact that the models have high Z_0 (0.020-0.025) and quite small Y_0 (0.24-0.26) leads us to doubt their validity. Taking a high Z_0 increases the M of the calibrated model. In this study, we set Z_0 = 0.0177. The model we obtained with M = 0.97 $M_\odot$ and R = 1.10 $R_\odot$ is in good agreement with observational constraints. For this well-fitting model, Y_0 is 0.2825. The $\Delta\nu$, ν_0, and $\delta\nu_{02}$ of this model are in excellent agreement with the observational values. The difference between the observational ν_0 and the model ν_0 (13 μHz) is much smaller than $\Delta\nu$ (116.9 μHz), while the model and observational $\delta\nu_{02}$ are close.

4.8.2 ϵ Tau (TIC 17554529): a member of the Hyades cluster

ϵ Tau is in a region of the HR diagram, where one cannot discriminate between RGB and RC stars. The period spacing $\Delta\Pi$ is a handy tool for asteroseismically discriminating between these two types of stars. An attempt by Arentoft et al. (2019) is unfortunately unsuccessful for the determination of $\Delta\Pi$. Modelling ϵ Tau as an RG star without mass loss yields as $M = 2.04 \pm 0.12$ $M_\odot$ and $t_9 = 0.98 \pm 0.18$ Gyr. Z_0 of this model is 0.0189.

4.8.3 KIC 6278762

This star has been the most challenging to model, with a match to the observations. The observational asteroseismic parameters are high-quality, and many [Fe/H] and $T_{\rm eff}$ values obtained from the spectrum based on SIMBAD data are consistent. A good fit is achieved only if the age is greater than the Milky Way's age. Especially with younger ages, the model's $T_{\rm eff}$ is higher than the observed value.

This star's $\delta\nu_{02}$=9.5 μHz. This means that this star is halfway through its MS lifetime. For the numerous models we constructed for this star, we obtained a relationship between $\delta\nu_{02}$ and M and α:

$$\delta\nu_{02} = -18.1 \pm 1.2 + (51.3 \pm 1.9)M - (5.55 \pm 0.19)\alpha. \quad (8)$$

When we set $\delta\nu_{02}$=9.5 μHz, we obtain the relationship between M and α. If we set $\alpha = \alpha_\odot$, M = 0.736 $M_\odot$. In this case, $T_{\rm eff}$ = 5400 – 5500 K. This model temperature is 350-450 K higher than the temperature obtained from the spectrum. In the model for which we obtained the best fit, M = 0.674 $M_\odot$ and α = 1.32. Unfortunately, this model's age also exceeds the age of the Galaxy.

This inconsistency reminds us once again of the necessity of opacity enhancement. It would be particularly appropriate to examine MS stars, which have masses lower than Kepler Legacy stars, in a separate study in this regard.

This system is also interesting for its five sub-earth-sized planets. If self-pollution occurred during planet formation in the disk, then we can obtain a solution by keeping Z free. In this case, for M = 0.737 $M_\odot$, Z_0 and age are found to be 0.0104 and 12.59 Gyr, respectively. Model results are given in Table **??**.

Although the self-pollution approach improves the model for this star, it does not achieve a good fit with the observations. The most likely options are opacity enhancement or planetary engulfment.

4.8.4 70 Vir (TIC 95473936)

Numerous spectral analyses have been conducted for this star. [Fe/H], $\log(g)$, and $T_{\rm eff}$ were determined in the analysis from 52 references in the SIMBAD database. According to these data, there are linear relationships between $T_{\rm eff}$ and $\log(g)$, and between [Fe/H] and $\log(g)$. $\log(g)$ = 3.90, determined by asteroseismic data. The most suitable data for this value is [Fe/H] = -0.09 and $T_{\rm eff}$ = 5501 K (Mahdi et al. 2016).

We obtained five different solutions that are close to each other. The properties of these models are listed in Table 2. Although the asteroseismic data are similar, only the input parameters M and Y_0 differ. Model masses range from 1.001 to 1.059 $M_\odot$, and Y_0 ranges from 0.25907 to 0.28556. Y_0 decreases as the model mass increases. These models have two notable features. First, the model $\nu_{\rm max}$ values are smaller than the observational $\nu_{\rm max}$ values. Second, the age remains almost constant across different values of M and Y_0. This demonstrates that such an analysis is successful in determining the age but limited in determining the chemical composition of such stars.

Table 1. Basic model properties of KIC 6278762.

M ($M_\odot$)	R ($R_\odot$)	Z_0	Z_s	Y_0	Y_s	α	$\Delta\nu$ (μHz)	$\delta\nu_{02}$ (μHz)	$T_{\rm eff}$ (K)	t_9 (Gyr)
0.737	0.750	0.0104	0.0089	0.2721	0.2329	1.7641	179.51	9.95	5068	11.71
0.700	0.735	0.0071	0.0058	0.2613	0.2154	1.4799	180.32	9.65	5042	13.46
0.674	0.721	0.0050	0.0039	0.2571	0.2065	1.3200	182.12	9.43	5042	14.58

Table 2. Basic properties of four interior models for TIC 95473936. Z_0 and α of the models are 0.0117 and 1.8311, respectively.

M $M_\odot$	R $R_\odot$	Y_0	$T_{\rm eff}$ K	L $L_\odot$	$\Delta\nu$ μHz	$\nu_{\rm max}$ μHz	t_9 Gyr
1.001	1.869	0.28556	5493	2.865	53.80	912	8.44
1.012	1.879	0.28056	5494	2.897	53.67	910	8.39
1.034	1.897	0.27056	5498	2.963	53.61	908	8.29
1.045	1.907	0.26556	5499	2.995	53.48	906	8.25
1.059	1.919	0.25907	5499	3.037	53.33	904	8.19
Obs.	——	——	5501	3.038	53.67	939	——

The star is close to $L_{\rm max}$ in the SG. It appears 200 K colder than that point. The TIC catalog gives L = 3.038 ± 0.081 $L_\odot$, and the model with the best fit for this luminosity has a mass of 1.059. Table 2 demonstrates the significant strengths of asteroseismic modeling. While we can determine the age quite precisely, a good estimate of the chemical composition also requires a precise measurement of the observed luminosity. For this example star, Z_0 = 0.0117 and Y_0 = 0.25907.

4.8.5 KIC 10963065

We calculated the reference frequencies for this star from its oscillation frequencies. The reference frequencies of the model we obtained are in excellent agreement with the observational ones.The model's M, R, and $T_{\rm eff}$ are in excellent agreement with the values calculated by Yıldız, Çelik Orhan, & Kayhan (2019).

4.8.6 KIC 4143755

This host is one of the lowest-mass stars in our catalog. SIMBAD data for this system are generally consistent. However, there is a significant difference between the model and spectral $T_{\rm eff}$s. Davies et al. (2016) gives $T_{\rm eff}$ = 5622 and [Fe/H] = -0.4. The majority of the SIMBAD data agree with these values: $T_{\rm eff}$ = 5600 K and [Fe/H] = -0.5 dex (Z_s = 0.00424). Obtaining a suitable fit with these values is difficult, and since the age is greater than the age of the Galaxy, our grid is insufficient. Our data is $T_{\rm eff}$ = 5746 K and [Fe/H] = -0.35 dex (Z_s = 0.00599). With these values and using $\Delta\nu$=77.2 μHz data, we obtained a model that agrees well with the observations by applying Method DZT: (M, R, Z_0, t_9, $T_{\rm eff}$)=(0.9078, 1.4210, 0.00819, 11.127, 5748). α and Y_0 of this model are 1.5652 and 0.26348, respectively. The observational reference frequencies of this host star are quite uncertain. There are only 5 points on the $\Delta\nu$-ν plot. In the models, $\nu_0 \sim$ 1500 and ν_1=1126 μHz.

4.8.7 KIC 8866102

Spectroscopic data for this host show significant scatter. In this case, we can apply the MinZ method to KIC 8866102. We calculated the $\Delta\nu$ of this star directly from the frequencies as 84.2 μHz. It is given as 83.6 μHz in the literature. For the MinZ method, χ^2 is computed as in Örtel et al. (2025). In Fig.10a, b, and c, $\log(\chi^2)$ is plotted with respect to M, Z, and $\log g$, respectively. In all of the panels, χ^2 is minimum at a single value of the horizontal axis. According to the MinZ method, (M, Z, $\log g$) = (1.26, 0.018, 4.263). For a solar-like oscillating star with precise observational asteroseismic data, we obtain a unique model for the host star.

4.8.8 TIC 302372658

When we use L=29.605 $L_\odot$, $\Delta\nu$=5.64 μHz and Z_s=0.0104 as constraints, we obtain the model parameters: (M, R, Z_0, t_9, $T_{\rm eff}$)=(1.14,8.60,0.0105, 6.14,4645). Observational $T_{\rm eff}$ is about 50 K greater than the model value.

4.8.9 TIC 200093173

Using L=6.911 $L_\odot$, $\Delta\nu$=37.71 μHz, and Z_s=0.02932 as constraints, we obtain the following model parameters: (M, R, Z_0, t_9, $T_{\rm eff}$)=(1.52, 2.74,0.0294, 2.82, 5578). Observational $T_{\rm eff}$ is close to the model value.

If we take Z_s=0.038, then we obtain (M, R, Z_0, t_9, $T_{\rm eff}$)=(1.53, 2.74,0.038, 2.53, 5673).

4.8.10 TIC 277890728

This star has a high Li abundance, A(Li)=2.65 (Delgado Mena et al. 2014). It is located in the region of the HR diagram where L is at its maximum after TAMS. In this case, α becomes irrelevant in the $T_{\rm eff}$ calibration. By changing Y_0, we calibrate both L and $T_{\rm eff}$. In Fig. 11, the evolution traces of three different models constructed with three different Y_0s are plotted in HRD. The model parameters that best match the observed properties of the star are as follows: M = 1.26 $M_\odot$, R = 1.97 $R_\odot$, Y_0 = 0.3109, Z_0 = 0.0319, and t_9 = 4.88 Gyr (see Table A2).

4.8.11 TIC 284181945

The model parameters we obtained by applying the DZT method are: (M, R, Z_0, t_9, $T_{\rm eff}$)=(1.8431, 10.6826, 0.01637, 0.7991, 4695). The $T_{\rm eff}$ is about 200 K higher. The $\Delta\Pi_1$ value for this star was found to be 303.96 ± 0.30 s by Lin, Qian, & Zhu (2024a). According to $\Delta\nu$ and $\Delta\Pi_1$, TIC 284181945 is an RC star. In Table A2, the values for an RG model are listed.

4.8.12 TIC 38828538 (HD 29399)

This host is an RG star (Lin, Qian, & Zhu 2024a). L is given by Pezzotti et al. (2022) as 10.04 $L_\odot$. 3 separate solutions: 1)$L_{\rm mod}$=10.04, 2)$L_{\rm mod}$=11.6681, 3) $T_{\rm eff}$=4845 K (L=12.626 $L_\odot$).

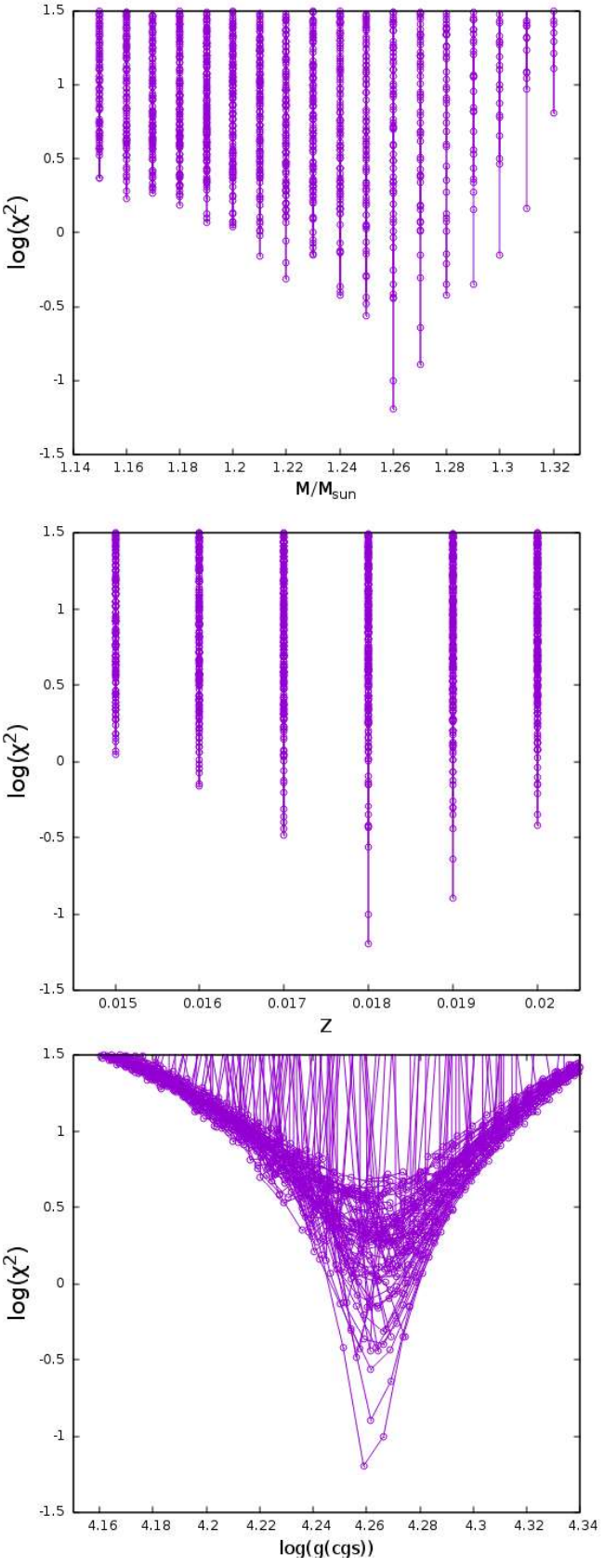

Figure 10. $\log(\chi^2)$ is plotted with respect to M (upper panel), Z (middle panel), and $\log(g)$ (lower panel) for KIC 8866102. For each of the parameters, $\log(\chi^2)$ is minimized at a single point.

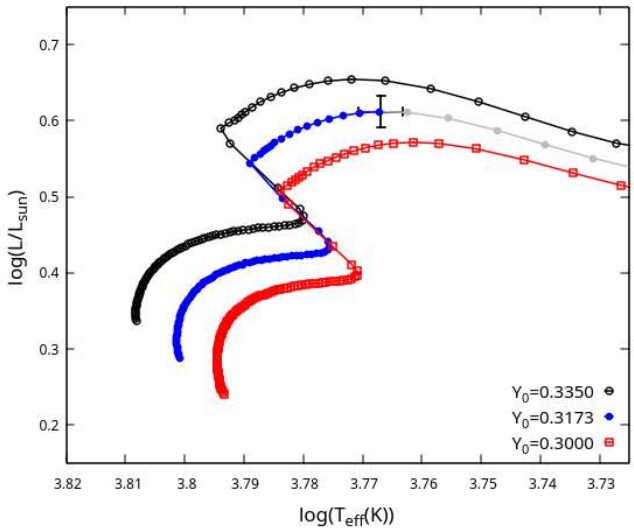

Figure 11. HRD of TIC 277890728 for the three models with different Y_0. The circle, filled circle, and box show the models with Y_0=0.3350, 0.3173, and 0.3000, respectively. The best model is with Y_0=0.3173

Table 3. Basic properties of the models constructed for TIC 38828538.

M ($M_\odot$)	R ($R_\odot$)	Z_0	t_9 (Gyr)	$T_{\rm eff}$ (K)
1.1631	4.6914	0.01856	6.7000	4738
1.2800	4.7100	0.01860	4.6600	4787
1.3663	4.9202	0.01868	3.7306	4806
1.4907	5.0431	0.01861	2.8387	4845
1.1394	4.4591	—	—	—

$\Delta\Pi_1$ = 83.55 ± 0.09 s (Lin, Qian, & Zhu 2024a). The host is an RG star.

When the difference between $T_{\rm mod}$ and $T_{\rm eff}$ was large, we obtained solutions with different L values to test the uncertainty level in the luminosity. These solutions are listed in Table **??**. $T_{\rm mod}$ increases with increasing L. When $L_{\rm mod}$12.6 $L_\odot$, $T_{\rm mod}$ and $T_{\rm eff}$ are equal. In this case, because the mass increases significantly, there are substantial age differences. The last row of the table shows M and R calculated from corrected scaling relations. $\Delta\nu$ of the model with M = 1.28 $M_\odot$ is in good agreement with the observed value. The difference between $T_{\rm mod}$ and $T_{\rm eff}$ is about 58 K for this model.

4.8.13 TIC 136916387

This star is interesting. It is near the main sequence and, according to the data, it is an old star. According to our model, it is 12.63 Gyr old. However, $Z_{\rm s}$ and Z_0 are approximately 0.0073 and 0.0093, respectively. This Z_0 is high for this age. Although the spectroscopic data in the SIMBAD database are quite scattered, it can be argued that this star exhibits interesting properties, such as chemical pollution. Lower [Fe/H] values have also been measured, but model calibration is complicated due to this low metallicity ($T_{\rm eff}$, [Fe/H])=(5700, -0.28) (Chavero et al. 2019). We obtain the best model with Z_0 = 0.0079. $T_{\rm eff}$ and $\Delta\nu$ of this model are in perfect agreement with the observed values.

4.8.14 TIC 233008631

TIC 233008631 has the smallest values for $\Delta\nu$ and ν_{max} among the hosts. For such stars, asteroseismic modelling is complex because the frequencies of only a few modes can be calculated using the ADIPLS package. Therefore, $\Delta\nu$ can only be calculated over a narrow range.

5 CONCLUSIONS

Asteroseismology is essential for understanding the internal structure of stars and constraining their fundamental parameters. Using quantities such as $\Delta\nu$, ν_{max}, and $\delta\nu_{02}$, stellar properties can be determined with much higher precision than with other methods. In recent years, the growing number of solar-like oscillating host stars has further strengthened the link between asteroseismology and exoplanet research, enabling the two fields to advance together.

In this study, we compiled data on 127 host stars (and six candidates) from the literature and constructed interior models of these stars using the MESA code. Rather than applying a single method, we developed multiple approaches based on the available data and their associated uncertainties. We used $\Delta\nu$ and Z_s as constraints in all the methods we implemented. Additionally, we included one or more of $\delta\nu_{02}$, ν_0, ν_1, L, T_{eff}, or R as constraints in the applied methods, depending on the sensitivity of the data and their compatibility with other data.

Two key results emerged from our models. First, with only a few exceptions, the majority of host stars have an initial metallicity (Z_0) greater than 0.008 (Fig. 6). This suggests that the threshold condition for planet formation is $Z_0 \approx 0.008$; if the metallicity of a host star is below this value, no planet formation is observed. Second, the age-metallicity relationship is quite variable. Both old and young stars can be metal-poor. For the most metal-rich stars of their time, the age-metallicity relationship appears linear up to $t_9 = 6$ Gyr. When $t_9 < 6$ Gyr, it seems to remain constant in the range $Z_0 = 0.008$-0.033. These results provide important insights into the chemical evolution of the Galactic disk.

Only one host clearly stands out: KIC 6278762. The model that best fits the observational data has a small mass and an age greater than the age of the Galaxy. A smaller model age would require a larger Z_0. In this case, the age decreases as the mass increases. In the context of this star, self-pollution in planetary systems can be discussed. Another option is opacity enhancement, which is thought to be particularly important for low-mass stars.

For the solar-like oscillating KIC 8866102 with precise observational asteroseismic data ($\Delta\nu$, ν_0, ν_1) and Z_s, we apply the MinZ method (Fig. 10) developed by (Örtel et al. 2025). We obtain a unique model for the host star. We could not apply this method to more stars due to the large number of models required.

Another important outcome of this study is the discovery of a relationship between Z_0 and the observed Z_s for the hosts. For the input parameter Z_0 used in the models, we derive a useful expression as a function of stellar mass, radius, and Z_s. This expression can be used to estimate Z_0 by accounting for the decrease in surface metallicity caused by microscopic diffusion.

The radius of a planet is mainly dependent on its mass. It is known that the incident flux, in particular, has a significant effect on gas giants. When using irradiation energy per gram per second rather than flux, we obtain a one-to-one relationship for the radius. We show for the first time that R_p depends not only on M_p and l_-, but also on one of the orbital parameters (P or a). Interestingly, our expression provides radius predictions for all planets, whether they are hot-jovian or terrestrial planets, including non-transiting planets.

This study provides the fundamental parameters of 127 solar-like oscillating host stars and their planets, establishing an essential catalog in the literature. These systems serve as natural laboratories for understanding star–planet evolution and for investigating planet formation and disk evolution. The results offer valuable insights into key questions in both asteroseismology and exoplanet research, while laying a solid foundation for future studies.

Extended data for planetary systems are provided in NASA Exoplanet Archive (Akeson et al. 2013) and TEPCat (Southworth 2011). It may be useful to create a continuously updated catalog of planetary systems with solar-like oscillating hosts using machine learning or to add asteroseismic data to existing catalogs.

ACKNOWLEDGEMENTS

This work is supported by the Scientific and Technological Research Council of Turkey (TÜBİTAK: 122F107).

DATA AVAILABILITY

The data underlying this article will be shared on reasonable request to the corresponding author.

REFERENCES

Abdurro'uf, Accetta K., Aerts C., Silva Aguirre V., Ahumada R., Ajgaonkar N., Filiz Ak N., et al., 2022, ApJS, 259, 35. doi:10.3847/1538-4365/ac4414

Adamów M., Niedzielski A., Kowalik K., Villaver E., Wolszczan A., Maciejewski G., Gromadzki M., 2018, A&A, 613, A47. doi:10.1051/0004-6361/201732161

Addison B. C., Wright D. J., Nicholson B. A., Cale B., Mocnik T., Huber D., Plavchan P., et al., 2021, MNRAS, 502, 3704. doi:10.1093/mnras/staa3960

Aguilera-Gómez C., Jones M. I., Chanamé J., 2023, A&A, 670, A73. doi:10.1051/0004-6361/202244518

Aguilera-Gómez C., Ramírez I., Chanamé J., 2018, A&A, 614, A55. doi:10.1051/0004-6361/201732209

Akeson R. L., Chen X., Ciardi D., Crane M., Good J., Harbut M., Jackson E., et al., 2013, PASP, 125, 989. doi:10.1086/672273

Arentoft T., Grundahl F., White T. R., Slumstrup D., Handberg R., Lund M. N., Brogaard K., et al., 2019, A&A, 622, A190. doi:10.1051/0004-6361/201834690

Appourchaux T., Chaplin W. J., García R. A., Gruberbauer M., Verner G. A., Antia H. M., Benomar O., et al., 2012, A&A, 543, A54. doi:10.1051/0004-6361/201218948

Arentoft T., Grundahl F., White T. R., Slumstrup D., Handberg R., Lund M. N., Brogaard K., et al., 2019, A&A, 622, A190. doi:10.1051/0004-6361/201834690

Asplund M., Grevesse N., Sauval A. J., Scott P., 2009, ARA&A, 47, 481. doi:10.1146/annurev.astro.46.060407.145222

Baglin A., Auvergne M., Barge P., Deleuil M., Catala C., Michel E., Weiss W., et al., 2006, ESASP, 1306, 33

Baines E. K., Armstrong J. T., van Belle G. T., 2013, ApJL, 771, L17. doi:10.1088/2041-8205/771/1/L17

Baines E. K., McAlister H. A., ten Brummelaar T. A., Sturmann J., Sturmann L., Turner N. H., Ridgway S. T., 2009, ApJ, 701, 154. doi:10.1088/0004-637X/701/1/154

Ball W. H., Chaplin W. J., Nielsen M. B., González-Cuesta L., Mathur S., Santos Â. R. G., García R., et al., 2020, MNRAS, 499, 6084. doi:10.1093/mnras/staa3190

Ball W. H., Gizon L., 2014, A&A, 568, A123. doi:10.1051/0004-6361/201424325

Barclay T., Rowe J. F., Lissauer J. J., Huber D., Fressin F., Howell S. B., Bryson S. T., et al., 2013, Natur, 494, 452. doi:10.1038/nature11914
Barbato D., Sozzetti A., Desidera S., Damasso M., Bonomo A. S., Giacobbe P., Colombo L. S., et al., 2018, A&A, 615, A175. doi:10.1051/0004-6361/201832791
Batalha N. M., Borucki W. J., Bryson S. T., Buchhave L. A., Caldwell D. A., Christensen-Dalsgaard J., Ciardi D., et al., 2011, ApJ, 729, 27. doi:10.1088/0004-637X/729/1/27
Batalha N. M., Rowe J. F., Bryson S. T., Barclay T., Burke C. J., Caldwell D. A., Christiansen J. L., et al., 2013, ApJS, 204, 24. doi:10.1088/0067-0049/204/2/24
Beard C., Robertson P., Giovinazzi M. R., Murphy J. M. A., Ford E. B., Halverson S., Han T., et al., 2024, AJ, 168, 149. doi:10.3847/1538-3881/ad6b22
Beck P. G., Hambleton K., Vos J., Kallinger T., Bloemen S., Tkachenko A., García R. A., et al., 2014, A&A, 564, A36. doi:10.1051/0004-6361/201322477
Beck P. G., Grossmann D. H., Steinwender L., Schimak L. S., Muntean N., Vrard M., Patton R. A., et al., 2024, A&A, 682, A7. doi:10.1051/0004-6361/202346810
Benbakoura M., Gaulme P., McKeever J., Sekaran S., Beck P. G., Spada F., Jackiewicz J., et al., 2021, A&A, 648, A113. doi:10.1051/0004-6361/202037783
Benedict G. F., McArthur B. E., Nelan E. P., Wittenmyer R., Barnes R., Smotherman H., Horner J., 2022, AJ, 163, 295. doi:10.3847/1538-3881/ac6ac8
Berger T. A., Huber D., Gaidos E., van Saders J. L., 2018, ApJ, 866, 99. doi:10.3847/1538-4357/aada83
Böhm-Vitense E., 1958, Zeitschrift für Astrophysik, 46, 108
Bonfanti A., Ortolani S., Piotto G., Nascimbeni V., 2015, A&A, 575, A18. doi:10.1051/0004-6361/201424951
Bonomo A. S., Borsato L., Rajpaul V. M., Zeng L., Damasso M., Hara N. C., Cretignier M., et al., 2025, arXiv, arXiv:2502.07996. doi:10.48550/arXiv.2502.07996
Bonomo A. S., Dumusque X., Massa A., Mortier A., Bongiolatti R., Malavolta L., Sozzetti A., et al., 2023, A&A, 677, A33.
Borgniet S., Lagrange A.-M., Meunier N., Galland F., 2017, A&A, 599, A57. doi:10.1051/0004-6361/201628805
Borucki W. J., Koch D., Basri G., Batalha N., Brown T., Caldwell D., Caldwell J., et al., 2010, Sci, 327, 977. doi:10.1126/science.1185402
Borucki W. J., Koch D. G., Brown T. M., Basri G., Batalha N. M., Caldwell D. A., Cochran W. D., et al., 2010, ApJL, 713, L126. doi:10.1088/2041-8205/713/2/L126
Bouchy F., Bazot M., Santos N. C., Vauclair S., Sosnowska D., 2005, A&A, 440, 609. doi:10.1051/0004-6361:20052697
Bressan A., Marigo P., Girardi L., Salasnich B., Dal Cero C., Rubele S., Nanni A., 2012, MNRAS, 427, 127. doi:10.1111/j.1365-2966.2012.21948.x
Brewer J. M., Fischer D. A., Valenti J. A., Piskunov N., 2017, ApJS, 230, 12. doi:10.3847/1538-4365/aa6d5a
Brewer J. M., Fischer D. A., Valenti J. A., Piskunov N., 2016, ApJS, 225, 32. doi:10.3847/0067-0049/225/2/32
Brewer J. M., Fischer D. A., 2018, ApJS, 237, 38. doi:10.3847/1538-4365/aad501
Brogaard K., Jessen-Hansen J., Handberg R., Arentoft T., Frandsen S., Grundahl F., Bruntt H., et al., 2016, AN, 337, 793. doi:10.1002/asna.201612374
Brogaard K., Hansen C. J., Miglio A., Slumstrup D., Frandsen S., Jessen-Hansen J., Lund M. N., et al., 2018, MNRAS, 476, 3729. doi:10.1093/mnras/sty268
Brogaard K., Arentoft T., Slumstrup D., Grundahl F., Lund M. N., Arndt L., Grund S., et al., 2022, A&A, 668, A82. doi:10.1051/0004-6361/202244345
Brown, T.M., Gilliland R.L., Noyes, R.W., Ramsey, L.W., 1991, ApJ, 368, 599
Brown T. M., Latham D. W., Everett M. E., Esquerdo G. A., 2011, AJ, 142, 112. doi:10.1088/0004-6256/142/4/112
Burke C. J., Bryson S. T., Mullally F., Rowe J. F., Christiansen J. L., Thompson S. E., Coughlin J. L., et al., 2014, ApJS, 210, 19. doi:10.1088/0067-0049/210/2/19
Butler R. P., Wright J. T., Marcy G. W., Fischer D. A., Vogt S. S., Tinney C. G., Jones H. R. A., et al., 2006, ApJ, 646, 505. doi:10.1086/504701
Campante T. L., Barclay T., Swift J. J., Huber D., Adibekyan V. Z., Cochran W., Burke C. J., et al., 2015, ApJ, 799, 170. doi:10.1088/0004-637X/799/2/170
Campante T. L., Corsaro E., Lund M. N., Mosser B., Serenelli A., Veras D., Adibekyan V., et al., 2019, ApJ, 885, 31. doi:10.3847/1538-4357/ab44a8
Carter J. A., Agol E., Chaplin W. J., Basu S., Bedding T. R., Buchhave L. A., Christensen-Dalsgaard J., et al., 2012, Sci, 337, 556. doi:10.1126/science.1223269
Chaplin W. J., Basu S., Huber D., Serenelli A., Casagrande L., Silva Aguirre V., Ball W. H., et al., 2014, ApJS, 210, 1. doi:10.1088/0067-0049/210/1/1
Chaplin W. J., Sanchis-Ojeda R., Campante T. L., Handberg R., Stello D., Winn J. N., Basu S., et al., 2013, ApJ, 766, 101. doi:10.1088/0004-637X/766/2/101
Charbonnel C., Lagarde N., Jasniewicz G., North P. L., Shetrone M., Krugler Hollek J., Smith V. V., et al., 2020, A&A, 633, A34. doi:10.1051/0004-6361/201936360
Chavero C., de la Reza R., Ghezzi L., Llorente de Andrés F., Pereira C. B., Giuppone C., Pinzón G., 2019, MNRAS, 487, 3162. doi:10.1093/mnras/stz1496
Chen R. E., Jiang J. H., Rosen P. E., Fahy K. A., Chen Y., 2023, Galaxies, 11, 112. doi:10.3390/galaxies11060112
Christensen-Dalsgaard J., 1993, ASPC, 42, 347
Christensen-Dalsgaard J., 1988, in Advances in Helio- and Asteroseismology, Aarhus, Denmark, July 11-17, 1986. Editors Christensen-Dalsgaard J. and Frandsen, S., IAU Symp. 123, Dordrecht: D. Reidel Publishing Co., p.295
Christensen-Dalsgaard J., 2008, ApSS, 316, 113
Coughlin J. L., Mullally F., Thompson S. E., Rowe J. F., Burke C. J., Latham D. W., Batalha N. M., et al., 2016, ApJS, 224, 12. doi:10.3847/0067-0049/224/1/12
Davies G. R., Silva Aguirre V., Bedding T. R., Handberg R., Lund M. N., Chaplin W. J., Huber D., et al., 2016, MNRAS, 456, 2183. doi:10.1093/mnras/stv2593
Davies G. R., Chaplin W. J., Farr W. M., García R. A., Lund M. N., Mathis S., Metcalfe T. S., et al., 2015, MNRAS, 446, 2959. doi:10.1093/mnras/stu2331
Deheuvels S., Brandão I., Silva Aguirre V., Ballot J., Michel E., Cunha M. S., Lebreton Y., et al., 2016, A&A, 589, A93. doi:10.1051/0004-6361/201527967
Deka-Szymankiewicz B., Niedzielski A., Adamczyk M., Adamów M., Nowak G., Wolszczan A., 2018, A&A, 615, A31. doi:10.1051/0004-6361/201731696
Delgado Mena E., Israelian G., González Hernández J. I., Sousa S. G., Mortier A., Santos N. C., Adibekyan V. Z., et al., 2014, A&A, 562, A92. doi:10.1051/0004-6361/201321493
Delrez L., Ehrenreich D., Alibert Y., Bonfanti A., Borsato L., Fossati L., Hooton M. J., et al., 2021, NatAs, 5, 775. doi:10.1038/s41550-021-01381-5
Desort M., Lagrange A.-M., Galland F., Beust H., Udry S., Mayor M., Lo Curto G., 2009, A&A, 499, 623. doi:10.1051/0004-6361/200810241e
D'Orazi V., Desidera S., Gratton R. G., Lanza A. F., Messina S., Andrievsky S. M., Korotin S., et al., 2017, A&A, 598, A19. doi:10.1051/0004-6361/201629283
Di Mauro M. P., Reda R., Mathur S., García R. A., Buzasi D. L., Corsaro E., Benomar O., et al., 2022, ApJ, 940, 93. doi:10.3847/1538-4357/ac8f44
Dressing C. D., Charbonneau D., Dumusque X., Gettel S., Pepe F., Collier Cameron A., Latham D. W., et al., 2015, ApJ, 800,
Dubber S. C., Mortier A., Rice K., Nava C., Malavolta L., Giles H., Coffinet A., et al., 2019, MNRAS, 490, 5103. doi:10.1093/mnras/stz2856
Feng F., Butler R. P., Vogt S. S., Clement M. S., Tinney C. G., Cui K., Aizawa M., et al., 2022, ApJS, 262, 21. doi:10.3847/1538-4365/ac7e57
Ferguson, J.W., Alexander, D.R., Allard, F., Barmanu, T., et al. 2005, ApJ, 623, 585
Fischer D., Driscoll P., Isaacson H., Giguere M., Marcy G. W., Valenti J., Wright J. T., et al., 2009, ApJ, 703, 1545. doi:10.1088/0004-637X/703/2/1545
Frandsen S., Lehmann H., Hekker S., Southworth J., Debosscher J., Beck

P., Hartmann M., et al., 2013, A&A, 556, A138. doi:10.1051/0004-6361/201321817
Frasca A., Molenda-Żakowicz J., De Cat P., Catanzaro G., Fu J. N., Ren A. B., Luo A. L., et al., 2016, A&A, 594, A39. doi:10.1051/0004-6361/201628337
Forsberg R., Ryde N., Jönsson H., Rich R. M., Johansen A., 2022, A&A, 666, A125. doi:10.1051/0004-6361/202244013
Fulton B. J., Petigura E. A., 2018, AJ, 156, 264. doi:10.3847/1538-3881/aae828
Gaia Collaboration, Brown A. G. A., Vallenari, A., Prusti, T., de Bruijne, J.H.J., et al., 2018, A&A, 616, A1
Gaia Collaboration, 2020, yCat, 1350
Gaia Collaboration, Brown A. G. A., Vallenari, A., Prusti, T., de Bruijne, J.H.J., et al., 2021, A&A, 649, A1
Gaia Collaboration, Brown A. G. A., Vallenari A., Prusti T., de Bruijne J. H. J., Babusiaux C., Biermann M., et al., 2021, A&A, 649, A1. doi:10.1051/0004-6361/202039657
Gaia Collaboration, Brown A. G. A., Vallenari A., Prusti T., de Bruijne J. H. J., Babusiaux C., Bailer-Jones C. A. L., et al., 2018, A&A, 616, A1. doi:10.1051/0004-6361/201833051
Gajdoš P., Vaňko M., Parimucha Š., 2019, RAA, 19, 041. doi:10.1088/1674-4527/19/3/41
Gaulme P., McKeever J., Jackiewicz J., Rawls M. L., Corsaro E., Mosser B., Southworth J., et al., 2016, ApJ, 832, 121. doi:10.3847/0004-637X/832/2/121
Gaulme P., Jackiewicz J., Spada F., Chojnowski D., Mosser B., McKeever J., Hedlund A., et al., 2020, A&A, 639, A63. doi:10.1051/0004-6361/202037781
Gaulme P., Borkovits T., Appourchaux T., Pavlovski K., Spada F., Gehan C., Ong J., et al., 2022, A&A, 668, A173. doi:10.1051/0004-6361/202244373
Ghezzi L., Montet B. T., Johnson J. A., 2018, ApJ, 860, 109. doi:10.3847/1538-4357/aac37c
Gilliland R. L., Marcy G. W., Rowe J. F., Rogers L., Torres G., Fressin F., Lopez E. D., et al., 2013, ApJ, 766, 40. doi:10.1088/0004-637X/766/1/40
Giguere M. J., Fischer D. A., Howard A. W., Johnson J. A., Henry G. W., Wright J. T., Marcy G. W., et al., 2012, ApJ, 744, 4. doi:10.1088/0004-637X/744/1/4
Gizon L., Ballot J., Michel E., Stahn T., Vauclair G., Bruntt H., Quirion P.-O., et al., 2013, PNAS, 110, 13267. doi:10.1073/pnas.1303291110
Gonzalez G., Carlson M. K., Tobin R. W., 2010, MNRAS, 403, 1368. doi:10.1111/j.1365-2966.2009.16195.x
González-Álvarez E., Affer L., Micela G., Maldonado J., Carleo I., Damasso M., D'Orazi V., et al., 2017, A&A, 606, A51. doi:10.1051/0004-6361/201731124
Gratton R. G., Bragaglia A., Carretta E., Clementini G., Desidera S., Grundahl F., Lucatello S., 2003, A&A, 408, 529. doi:10.1051/0004-6361:20031003
Grieves N., Ge J., Thomas N., Willis K., Ma B., Lorenzo-Oliveira D., Queiroz A. B. A., et al., 2018, MNRAS, 481, 3244. doi:10.1093/mnras/sty2431
Grossmann D. H., Beck P. G., Mathur S., Johnston C., Godoy-Rivera D., Zinn J. C., Cassisi S., et al., 2025, arXiv, arXiv:2501.09018. doi:10.48550/arXiv.2501.09018
Grunblatt S. K., Huber D., Gaidos E., Lopez E. D., Barclay T., Chontos A., Sinukoff E., et al., 2018, ApJL, 861, L5. doi:10.3847/2041-8213/aacc67
Harakawa H., Sato B., Omiya M., Fischer D. A., Hori Y., Ida S., Kambe E., et al., 2015, ApJ, 806, 5. doi:10.1088/0004-637X/806/1/5
Hatt E., Nielsen M. B., Chaplin W. J., Ball W. H., Davies G. R., Bedding T. R., Buzasi D. L., et al., 2023, A&A, 669, A67. doi:10.1051/0004-6361/202244579
Haywood R. D., Vanderburg A., Mortier A., Giles H. A. C., López-Morales M., Lopez E. D., Malavolta L., et al., 2018, AJ, 155, 203. doi:10.3847/1538-3881/aab8f3
Haywood R. D., Vanderburg A., Mortier A., Giles H. A. C., López-Morales M., Lopez E. D., Malavolta L., et al., 2018, AJ, 155, 203. doi:10.3847/1538-3881/aab8f
Hekker S., Debosscher J., Huber D., Hidas M. G., De Ridder J., Aerts C., Stello D., et al., 2010, ApJL, 713, L187. doi:10.1088/2041-8205/713/2/L187
Hekker S., Meléndez J., 2007, A&A, 475, 1003. doi:10.1051/0004-6361:20078233
Hill M. L., Kane S. R., Campante T. L., Li Z., Dalba P. A., Brandt T. D., White T. R., et al., 2021, AJ, 162, 211. doi:10.3847/1538-3881/ac1b31
Howell S. B., Sobeck C., Haas M., Still M., Barclay T., Mullally F., Troeltzsch J., et al., 2014, PASP, 126, 398. doi:10.1086/676406
Huang C. X., Burt J., Vanderburg A., Günther M. N., Shporer A., Dittmann J. A., Winn J. N., et al., 2018, ApJL, 868, L39. doi:10.3847/2041-8213/aaef91
Huber D., Zinn J., Bojsen-Hansen M., Pinsonneault M., Sahlholdt C., Serenelli A., Silva Aguirre V., et al., 2017, ApJ, 844, 102. doi:10.3847/1538-4357/aa75ca
Huber D., Chaplin W. J., Christensen-Dalsgaard J., Gilliland R. L., Kjeldsen H., Buchhave L. A., Fischer D. A., et al., 2013, ApJ, 767, 127. doi:10.1088/0004-637X/767/2/127
Huber D., Chaplin W. J., Chontos A., Kjeldsen H., Christensen-Dalsgaard J., Bedding T. R., Ball W., et al., 2019, AJ, 157, 245. doi:10.3847/1538-3881/ab1488
Huber D., White T. R., Metcalfe T. S., Chontos A., Fausnaugh M. M., Ho C. S. K., Van Eylen V., et al., 2022, AJ, 163, 79. doi:10.3847/1538-3881/ac3000
Huber D., Carter J. A., Barbieri M., Miglio A., Deck K. M., Fabrycky D. C., Montet B. T., et al., 2013, Sci, 342, 331. doi:10.1126/science.1242066
Iglesias C. A., Rogers F. J., 1993, ApJ, 412, 752. doi:10.1086/172958
Iglesias C.A., and Rogers F.J. 1996, ApJ, 464, 943
Jeong G., Lee B.-C., Han I., Omiya M., Izumiura H., Sato B., Harakawa H., et al., 2018, A&A, 610, A3. doi:10.1051/0004-6361/201629185
Jeong G., Lee B.-C., Park M.-G., Bang T.-Y., Han I., 2022, A&A, 662, A12. doi:10.1051/0004-6361/202142379
Jermyn A. S., Bauer E. B., Schwab J., Farmer R., Ball W. H., Bellinger E. P., Dotter A., et al., 2023, ApJS, 265, 15. doi:10.3847/1538-4365/acae8d
Jiang C., Bedding T. R., Stassun K. G., Veras D., Corsaro E., Buzasi D. L., Mikołajczyk P., et al., 2020, ApJ, 896, 65. doi:10.3847/1538-4357/ab8f29
Jofré E., Petrucci R., Saffe C., Saker L., Artur de la Villarmois E., Chavero C., Gómez M., et al., 2015, A&A, 574, A50. doi:10.1051/0004-6361/201424474
Johnson J. A., Clanton C., Howard A. W., Bowler B. P., Henry G. W., Marcy G. W., Crepp J. R., et al., 2011, ApJS, 197, 26. doi:10.1088/0067-0049/197/2/26
Johnson J. A., Bowler B. P., Howard A. W., Henry G. W., Marcy G. W., Isaacson H., Brewer J. M., et al., 2010, ApJL, 721, L153. doi:10.1088/2041-8205/721/2/L153
Jones M. I., Jenkins J. S., Bluhm P., Rojo P., Melo C. H. F., 2014, A&A, 566, A113. doi:10.1051/0004-6361/201323345
Jones M. I., Wittenmyer R., Aguilera-Gómez C., Soto M. G., Torres P., Trifonov T., Jenkins J. S., et al., 2021, A&A, 646, A131. doi:10.1051/0004-6361/202038555
Jones M. I., Jenkins J. S., Rojo P., Melo C. H. F., Bluhm P., 2015, A&A, 573, A3. doi:10.1051/0004-6361/201424771
Jones M. I., Jenkins J. S., Brahm R., Wittenmyer R. A., Olivares E. F., Melo C. H. F., Rojo P., et al., 2016, A&A, 590, A38. doi:10.1051/0004-6361/201628067
Johnson J. A., Payne M., Howard A. W., Clubb K. I., Ford E. B., Bowler B. P., Henry G. W., et al., 2011, AJ, 141, 16. doi:10.1088/0004-6256/141/1/16
Kjeldsen H., and Bedding T. R. 1995, A&A, 293, 87
Kjeldsen H., Bedding T. R., Christensen-Dalsgaard J., 2008, ApJL, 683, L175. doi:10.1086/591667
Kane S. R., Boyajian T. S., Henry G. W., Feng Y. K., Hinkel N. R., Fischer D. A., von Braun K., et al., 2015, ApJ, 806, 60. doi:10.1088/0004-637X/806/1/60
Kang W., Lee S.-G., Kim K.-M., 2011, ApJ, 736, 87. doi:10.1088/0004-637X/736/2/87
Kayhan C., Yıldız M., Çelik Orhan Z., 2019, MNRAS, 490, 1509. doi:10.1093/mnras/stz2634
Kuzuhara M., Tamura M., Kudo T., Janson M., Kandori R., Brandt T. D., Thalmann C., et al., 2013, ApJ, 774, 11. doi:10.1088/0004-637X/774/1/11
Lebzelter T., Wood P. R., 2011, A&A, 529, A137. doi:10.1051/0004-6361/201016319
Lee B.-C., Park M.-G., Lee S.-M., Jeong G., Oh H.-I., Han I., Lee J. W., et

al., 2015, A&A, 584, A79. doi:10.1051/0004-6361/201527076
Leleu A., Delisle J.-B., Udry S., Mardling R., Turbet M., Egger J. A., Alibert Y., et al., 2023, A&A, 669, A117. doi:10.1051/0004-6361/202244132
Li T., Li Y., Bi S., Bedding T. R., Davies G., Du M., 2022, ApJ, 927, 167. doi:10.3847/1538-4357/ac4fbf
Lin W.-X., Qian S.-B., Zhu L.-Y., 2024, ApJL, 971, L50. doi:10.3847/2041-8213/ad6c49
Lin W.-X., Qian S.-B., Zhu L.-Y., Liao W.-P., Li F.-X., 2024, AJ, 168, 27. doi:10.3847/1538-3881/ad4ffc
Lin W.-X., Qian S.-B., Zhu L.-Y., Liao W.-P., Li F.-X., Shi X.-D., Li L.-J., et al., 2025, ApJ, 978, 24. doi:10.3847/1538-4357/ad973c
Liu Y. J., Tan K. F., Wang L., Zhao G., Sato B., Takeda Y., Li H. N., 2014, ApJ, 785, 94. doi:10.1088/0004-637X/785/2/94
Luck R. E., 2017, AJ, 153, 21. doi:10.3847/1538-3881/153/1/21
Luhn J. K., Bastien F. A., Wright J. T., Johnson J. A., Howard A. W., Isaacson H., 2019, AJ, 157, 149. doi:10.3847/1538-3881/aaf5d0
Lund M. N., Silva Aguirre V., Davies G. R., Chaplin W. J., Christensen-Dalsgaard J., Houdek G., White T. R., et al., 2017, ApJ, 835, 172. doi:10.3847/1538-4357/835/2/172
Luque R., Trifonov T., Reffert S., Quirrenbach A., Lee M. H., Albrecht S., Fredslund Andersen M., et al., 2019, A&A, 631, A136. doi:10.1051/0004-6361/201936464
Mahdi D., Soubiran C., Blanco-Cuaresma S., Chemin L., 2016, A&A, 587, A131. doi:10.1051/0004-6361/201527472
Maldonado J., Villaver E., 2016, A&A, 588, A98. doi:10.1051/0004-6361/201527883
Marcy G. W., Isaacson H., Howard A. W., Rowe J. F., Jenkins J. M., Bryson S. T., Latham D. W., et al., 2014, ApJS, 210, 20. doi:10.1088/0067-0049/210/2/20
Marmier M., Ségransan D., Udry S., Mayor M., Pepe F., Queloz D., Lovis C., et al., 2013, A&A, 551, A90. doi:10.1051/0004-6361/201219639
Meléndez J., Asplund M., Alves-Brito A., Cunha K., Barbuy B., Bessell M. S., Chiappini C., et al., 2008, A&A, 484, L21. doi:10.1051/0004-6361:200809398
Ment K., Fischer D. A., Bakos G., Howard A. W., Isaacson H., 2018, AJ, 156, 213. doi:10.3847/1538-3881/aae1f5
Meschiari S., Laughlin G., Vogt S. S., Butler R. P., Rivera E. J., Haghighipour N., Jalowiczor P., 2011, ApJ, 727, 117. doi:10.1088/0004-637X/727/2/117
Metcalfe T. S., Chaplin W. J., Appourchaux T., García R. A., Basu S., Brandão I., Creevey O. L., et al., 2012, ApJL, 748, L10. doi:10.1088/2041-8205/748/1/L10
Metcalfe T. S., Buzasi D., Huber D., Pinsonneault M. H., van Saders J. L., Ayres T. R., Basu S., et al., 2023, AJ, 166, 167. doi:10.3847/1538-3881/acf1f7
Miglio A., Brogaard K., Stello D., Chaplin W. J., D'Antona F., Montalbán J., Basu S., et al., 2012, MNRAS, 419, 2077. doi:10.1111/j.1365-2966.2011.19859.x
Mills S. M., Howard A. W., Weiss L. M., Steffen J. H., Isaacson H., Fulton B. J., Petigura E. A., et al., 2019, AJ, 157, 145. doi:10.3847/1538-3881/ab0899
Molenda-Żakowicz J., Sousa S. G., Frasca A., Uytterhoeven K., Briquet M., Van Winckel H., Drobek D., et al., 2013, MNRAS, 434, 1422. doi:10.1093/mnras/stt1095
Montes D., González-Peinado R., Tabernero H. M., Caballero J. A., Marfil E., Alonso-Floriano F. J., Cortés-Contreras M., et al., 2018, MNRAS, 479, 1332. doi:10.1093/mnras/sty1295
Morton T. D., Bryson S. T., Coughlin J. L., Rowe J. F., Ravichandran G., Petigura E. A., Haas M. R., et al., 2016, ApJ, 822, 86. doi:10.3847/0004-637X/822/2/86
Naef D., Mayor M., Pepe F., Queloz D., Santos N. C., Udry S., Burnet M., 2001, A&A, 375, 205. doi:10.1051/0004-6361:20010841
Niedzielski A., Villaver E., Wolszczan A., Adamów M., Kowalik K., Maciejewski G., Nowak G., et al., 2015, A&A, 573, A36. doi:10.1051/0004-6361/201424399
Niedzielski A., Villaver E., Nowak G., Adamów M., Kowalik K., Wolszczan A., Deka-Szymankiewicz B., et al., 2016, A&A, 588, A62. doi:10.1051/0004-6361/201527869
Nielsen M. B., Ball W. H., Standing M. R., Triaud A. H. M. J., Buzasi D., Carboneau L., Stassun K. G., et al., 2020, A&A, 641, A25. doi:10.1051/0004-6361/202037461
Ortiz M., Reffert S., Trifonov T., Quirrenbach A., Mitchell D. S., Nowak G., Buenzli E., et al., 2016, A&A, 595, A55. doi:10.1051/0004-6361/201628791
Örtel S., Yıldız M., Çelik Orhan Z., 2025, MNRAS, 538, 844. doi:10.1093/mnras/staf140
O'Toole S., Tinney C. G., Butler R. P., Jones H. R. A., Bailey J., Carter B. D., Vogt S. S., et al., 2009, ApJ, 697, 1263. doi:10.1088/0004-637X/697/2/1263
Ottoni G., Udry S., Ségransan D., Buldgen G., Lovis C., Eggenberger P., Pezzotti C., et al., 2022, A&A, 657, A87. doi:10.1051/0004-6361/202040078
Paletou F., Böhm T., Watson V., Trouilhet J.-F., 2015, A&A, 573, A67. doi:10.1051/0004-6361/201424741
Pál A., Bakos G. Á., Torres G., Noyes R. W., Latham D. W., Kovács G., Marcy G. W., et al., 2008, ApJ, 680, 1450. doi:10.1086/588010
Paquette C., Pelletier C., Fontaine G., Michaud G., 1986, ApJS, 61, 177. doi:10.1086/191111
Pasquini L., Bonifacio P., Randich S., Galli D., Gratton R. G., 2004, A&A, 426, 651. doi:10.1051/0004-6361:20041254
Paxton B., Bildsten L., Dotter A., Herwig F., Lesaffre P. and Timmes F., 2011, ApJS, 192, 35
Paxton B., Cantiello M., Arras P., Bildsten L., Brown, E.F, et al., 2013, ApJS, 208, 42
Paxton B., Marchant P., Schwab J., Bauer E. B., Bildsten L., Cantiello M., Dessart L., et al., 2015, ApJS, 220, 15. doi:10.1088/0067-0049/220/1/15
Paxton B., Schwab J., Bauer E. B., Bildsten L., Blinnikov S., Duffell P., Farmer R., et al., 2018, ApJS, 234, 34. doi:10.3847/1538-4365/aaa5a8
Paxton B., Smolec R., Schwab J., Gautschy A., Bildsten L., Cantiello M., Dotter A., et al., 2019, ApJS, 243, 10. doi:10.3847/1538-4365/ab2241
Perdelwitz V., Trifonov T., Teklu J. T., Sreenivas K. R., Tal-Or L., 2024, A&A, 683, A125. doi:10.1051/0004-6361/202348263
Petigura E. A., Howard A. W., Marcy G. W., Johnson J. A., Isaacson H., Cargile P. A., Hebb L., et al., 2017, AJ, 154, 107. doi:10.3847/1538-3881/aa80de
Pezzotti C., Ottoni G., Buldgen G., Lyttle A., Eggenberger P., Udry S., Ségransan D., et al., 2022, A&A, 657, A89. doi:10.1051/0004-6361/202040080
Philipot F., Lagrange A.-M., Kiefer F., Rubini P., Delorme P., Chomez A., 2023, A&A, 678, A107. doi:10.1051/0004-6361/202346612
Pinsonneault M. H., Elsworth Y. P., Tayar J., Serenelli A., Stello D., Zinn J., Mathur S., et al., 2018, ApJS, 239, 32. doi:10.3847/1538-4365/aaebfd
Planck Collaboration, Aghanim N., Akrami Y., Ashdown M., Aumont J., Baccigalupi C., Ballardini M., et al., 2020, A&A, 641, A6. doi:10.1051/0004-6361/201833910
Rajpaul V. M., Buchhave L. A., Lacedelli G., Rice K., Mortier A., Malavolta L., Aigrain S., et al., 2021, MNRAS, 507, 1847. doi:10.1093/mnras/stab2192
Rawls M. L., Gaulme P., McKeever J., Jackiewicz J., Orosz J. A., Corsaro E., Beck P. G., et al., 2016, ApJ, 818, 108. doi:10.3847/0004-637X/818/2/108
Rice M., Brewer J. M., 2020, ApJ, 898, 119. doi:10.3847/1538-4357/ab9f96
Ricker G. R., Winn J. N., Vanderspek R., Latham D. W., Bakos G. Á., Bean J. L., Berta-Thompson Z. K., et al., 2015, JATIS, 1, 014003. doi:10.1117/1.JATIS.1.1.014003
Rosenthal L. J., Fulton B. J., Hirsch L. A., Isaacson H. T., Howard A. W., Dedrick C. M., Sherstyuk I. A., et al., 2021, ApJS, 255, 8. doi:10.3847/1538-4365/abe23c
Rowan D. M., Stanek K. Z., Kochanek C. S., Thompson T. A., Jayasinghe T., Blaum J., Fulton B. J., et al., 2024, arXiv, arXiv:2409.02983. doi:10.48550/arXiv.2409.02983
Rowe J. F., Bryson S. T., Marcy G. W., Lissauer J. J., Jontof-Hutter D., Mullally F., Gilliland R. L., et al., 2014, ApJ, 784, 45. doi:10.1088/0004-637X/784/1/45
Santos N. C., Sousa S. G., Mortier A., Neves V., Adibekyan V., Tsantaki M., Delgado Mena E., et al., 2013, A&A, 556, A150. doi:10.1051/0004-6361/201321286

Santos N. C., Israelian G., Mayor M., 2004, A&A, 415, 1153. doi:10.1051/0004-6361:20034469
Sato B., Omiya M., Wittenmyer R. A., Harakawa H., Nagasawa M., Izumiura H., Kambe E., et al., 2013, ApJ, 762, 9. doi:10.1088/0004-637X/762/1/9
Sato B., Toyota E., Omiya M., Izumiura H., Kambe E., Masuda S., Takeda Y., et al., 2008, PASJ, 60, 1317. doi:10.1093/pasj/60.6.1317
Saunders N., Grunblatt S. K., Huber D., Ong J. M. J., Schlaufman K. C., Hey D., Li Y., et al., 2025, AJ, 169, 75. doi:10.3847/1538-3881/ad9a87
Seager S., Mallén-Ornelas G., 2003, ApJ, 585, 1038. doi:10.1086/346105
Setiawan J., Rodmann J., da Silva L., Hatzes A. P., Pasquini L., von der Lühe O., de Medeiros J. R., et al., 2005, A&A, 437, L31. doi:10.1051/0004-6361:200500133
Sharma S., Stello D., Bland-Hawthorn J. et al. 2016, ApJ, 822, 15
Silva Aguirre V., Davies G. R., Basu S., Christensen-Dalsgaard J., Creevey O., Metcalfe T. S., Bedding T. R., et al., 2015, MNRAS, 452, 2127. doi:10.1093/mnras/stv1388
Skrutskie M. F., Cutri R. M., Stiening R., Weinberg M. D., Schneider S., Carpenter J. M., Beichman C., et al., 2006, AJ, 131, 1163. doi:10.1086/498708
Soto M. G., Jenkins J. S., Jones M. I., 2015, Msngr, 161, 24
Soto M. G., Jones M. I., Jenkins J. S., 2021, A&A, 647, A157. doi:10.1051/0004-6361/202039357
Soubiran C., Brouillet N., Casamiquela L., 2022, A&A, 663, A4. doi:10.1051/0004-6361/202142409
Sousa S. G., Santos N. C., Mortier A., Tsantaki M., Adibekyan V., Delgado Mena E., Israelian G., et al., 2015, A&A, 576, A94. doi:10.1051/0004-6361/201425227
Sousa S. G., Adibekyan V., Delgado-Mena E., Santos N. C., Andreasen D. T., Ferreira A. C. S., Tsantaki M., et al., 2018, A&A, 620, A58. doi:10.1051/0004-6361/201833350
Sousa S. G., Santos N. C., Mayor M., Udry S., Casagrande L., Israelian G., Pepe F., et al., 2008, A&A, 487, 373. doi:10.1051/0004-6361:200809698
Southworth J., 2011, MNRAS, 417, 2166. doi:10.1111/j.1365-2966.2011.19399.x
Stassun K. G., Collins K. A., Gaudi B. S., 2017, AJ, 153, 136. doi:10.3847/1538-3881/aa5df3
Stock S., Reffert S., Quirrenbach A., 2018, A&A, 616, A33. doi:10.1051/0004-6361/201833111
Sullivan, P. W., Winn, J.N., Berta-Thompson, Z.K., Charbonneau, D., Deming, D., et al., 2015, ApJ, 809, 77
Tassoul M., 1980, ApJS, 43, 469. doi:10.1086/190678
Tautvaišienė G., Mikolaitis Š., Drazdauskas A., Stonkutė E., Minkevičiūtė R., Pakštienė E., Kjeldsen H., et al., 2022, ApJS, 259, 45. doi:10.3847/1538-4365/ac50b
Teng H.-Y., Sato B., Kuzuhara M., Takarada T., Omiya M., Harakawa H., Izumiura H., et al., 2023, PASJ, 75, 1030. doi:10.1093/pasj/psad056
Teng H.-Y., Sato B., Takarada T., Omiya M., Harakawa H., Izumiura H., Kambe E., et al., 2022, PASJ, 74, 92. doi:10.1093/pasj/psab112
Teng H.-Y., Sato B., Takarada T., Omiya M., Harakawa H., Nagasawa M., Hasegawa R., et al., 2022, PASJ, 74, 1309. doi:10.1093/pasj/psac070
Themeßl N., Hekker S., Southworth J., Beck P. G., Pavlovski K., Tkachenko A., Angelou G. C., et al., 2018, MNRAS, 478, 4669. doi:10.1093/mnras/sty1113
Ting Y.-S., Conroy C., Rix H.-W., Cargile P., 2019, ApJ, 879, 69. doi:10.3847/1538-4357/ab2331
Trifonov T., Wollbold A., Kürster M., Eberhardt J., Stock S., Henning T., Reffert S., et al., 2022, AJ, 164, 156. doi:10.3847/1538-3881/ac7ce0
Tsantaki M., Sousa S. G., Santos N. C., Montalto M., Delgado-Mena E., Mortier A., Adibekyan V., et al., 2014, A&A, 570, A80. doi:10.1051/0004-6361/201424257
Valizadegan H., Martinho M. J. S., Wilkens L. S., Jenkins J. M., Smith J. C., Caldwell D. A., Twicken J. D., et al., 2022, ApJ, 926, 120. doi:10.3847/1538-4357/ac4399
Van Eylen V., Lund M. N., Silva Aguirre V., Arentoft T., Kjeldsen H., Albrecht S., Chaplin W. J., et al., 2014, ApJ, 782, 14. doi:10.1088/0004-637X/782/1/14
Venner A., Vanderburg A., Pearce L. A., 2021, AJ, 162, 12. doi:10.3847/1538-3881/abf932
Vernekar N., Lucatello S., Bragaglia A., Miglio A., Sanna N., Andreuzzi G., Frasca A., 2024, A&A, 684, A85. doi:10.1051/0004-6361/202348133
Wang L., Wang W., Wu Y., Zhao G., Li Y., Luo A., Liu C., et al., 2016, AJ, 152, 6. doi:10.3847/0004-6256/152/1/6
Wenger M., Ochsenbein F., Egret D., Dubois P., Bonnarel F., Borde S., Genova F., et al., 2000, A&AS, 143, 9. doi:10.1051/aas:2000332
Weiss L., Isaacson H., Howard A., Fulton B., Petigura E., Fabrycky D., Jontof-Hutter D., et al., 2024, DDA, 56, 202.07
Weiss L. M., Isaacson H., Howard A. W., Fulton B. J., Petigura E. A., Fabrycky D., Jontof-Hutter D., et al., 2024, ApJS, 270, 8. doi:10.3847/1538-4365/ad0cab
Wilson R. F., Cañas C. I., Majewski S. R., Cunha K., Smith V. V., Bender C. F., Mahadevan S., et al., 2022, AJ, 163, 128. doi:10.3847/1538-3881/ac3a06
Wittenmyer R. A., Endl M., Wang L., Johnson J. A., Tinney C. G., O'Toole S. J., 2011, ApJ, 743, 184. doi:10.1088/0004-637X/743/2/184
Wittenmyer R. A., Jones M. I., Zhao J., Marshall J. P., Butler R. P., Tinney C. G., Wang L., et al., 2017, AJ, 153, 51. doi:10.3847/1538-3881/153/2/51
Wittenmyer R. A., Liu F., Wang L., Casagrande L., Johnson J. A., Tinney C. G., 2016, AJ, 152, 19. doi:10.3847/0004-6256/152/1/19
Wittenmyer R. A., Johnson J. A., Butler R. P., Horner J., Wang L., Robertson P., Jones M. I., et al., 2016, ApJ, 818, 35. doi:10.3847/0004-637X/818/1/35
Wittenmyer R. A., Endl M., Cochran W. D., Levison H. F., Henry G. W., 2009, ApJS, 182, 97. doi:10.1088/0067-0049/182/1/97
Yıldız M., Doğan T., 2013, MNRAS, 430, 2029. doi:10.1093/mnras/stt028
Yıldız M., Çelik Orhan Z., Kayhan C., Turkoglu G. E., 2014, MNRAS, 445, 4395. doi:10.1093/mnras/stu2053
Yıldız M., 2015, RAA, 15, 2244. doi:10.1088/1674-4527/15/12/012
Yıldız M., Çelik Orhan Z., Kayhan C., 2016, MNRAS, 462, 1577. doi:10.1093/mnras/stw1709
Yıldız M., Çelik Orhan Z., Kayhan C., 2019, MNRAS, 489, 1753. doi:10.1093/mnras/stz2223
Yıldız M., Örtel S., 2021, MNRAS, 504, 2273. doi:10.1093/mnras/stab996
Yıldız M., 2023, MNRAS, 518, 5552. doi:10.1093/mnras/stac3464
Zhang J., Weiss L. M., Huber D., Blunt S., Chontos A., Fulton B. J., Grunblatt S., et al., 2021, AJ, 162, 89. doi:10.3847/1538-3881/ac0634
Zhang L.-. yun ., Su T., Misra P., Han X. L., Meng G., Pi Q., Yang J., 2023, ApJS, 264, 17. doi:10.3847/1538-4365/ac9b28
Zhang J., Qian S.-B., Wu Y., Zhou X., 2019, ApJS, 244, 43. doi:10.3847/1538-4365/ab442b
Zhou J., Bi S., Yu J., Li Y., Zhang X., Li T., Long L., et al., 2024, yCat, 227. J/ApJS/271/17
Xiao G.-Y., Liu Y.-J., Teng H.-Y., Wang W., Brandt T. D., Zhao G., Zhao F., et al., 2023, RAA, 23, 055022. doi:10.1088/1674-4527/accb7e
Xie J.-W., 2014, ApJS, 210, 25. doi:10.1088/0067-0049/210/2/25